

Supporting Information

for

Tetra-benzimidazoles flanking from divinyl-phenothiazine: AIEgens as aza-Michael acceptors in concentration-based responses to biogenic amine vapors

Sameer Singh,^a Kalyaneswar Mandal,^b and Manab Chakravarty*^a

^aDepartment of Chemistry, Birla Institute of Technology and Sciences, Pilani-Hyderabad Campus
Jawahar Nagar, Shamirpet, Hyderabad – 500078, India E-mail: manab@hyderabad.bits-pilani.ac.in

^bTata Institute of Fundamental Research Hyderabad 36/p Gopanpally, Hyderabad, Telangana – 500046,
India E-mail: kmandal@tifrh.res.in

Table of contents

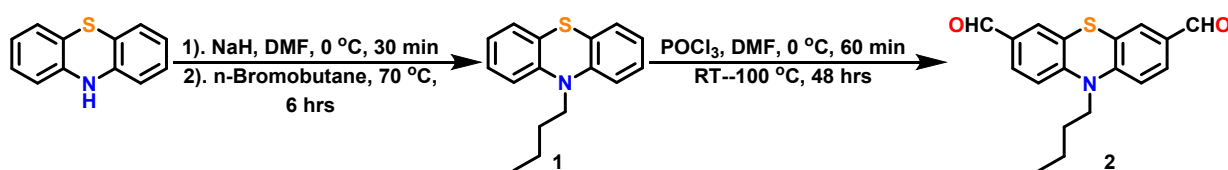
1. Standard technique and instruments employed	S2
2. Synthetic procedure and optimization.....	S2-9
2.1. Synthesis of 10-butyl-10H-phenothiazine-3,7-dicarbaldehyde (2)	
2.2. BIZM synthesis optimization using malonic acid	
2.3. BIZM synthesis optimization using malonamide	
2.4. Comparison of product (3) conversion using malonic acid vs malonamide	
2.5. Synthesis of Methyl 3,4-diamino-benzoate (4)	
2.6. General procedure for BIZM and its analogue synthesis	
2.7. General procedure for Probe and its analogue synthesis	
3. Spectroscopic study.....	S10-20
4. NMR and LCMS analysis for the reaction mechanism.....	S21-26
4.1. LCMS profile for the reduction of PBES-R and PBES-Y	
4.2. ¹ H-NMR study for PBES, PBES-R and PBES-Y	
5. PXRD data.....	S26
6. NMR and HRMS data.....	S27-44
7. References.....	S44

1. Standard techniques and instruments employed

Analytical reverse phase (RP) HPLC was performed on an Agilent 1260 infinity II HPLC using a reverse phase-silica bound column Agilent Zorbax 300SB-C3 (5 μ m), 4.6 x 150 mm. The high-resolution ESI mass spectra were performed on an Agilent 1290 infinity II/6530 Q-TOF LC-MS (capillary voltage 4000 V, Gas temperature 325 $^{\circ}$ C, Nebulizer pressure 50 psi, drying gas flow 11 L/min, fragmentor voltage 200V, skimmer voltage 60 V). The electronic absorption spectra were recorded with UV3600Plus (Shimadzu). The FL spectra was recorded using a Hitachi spectrofluorometer (F7000) using a 1 cm path-length quartz cuvette. Origin Pro 2023b (10.05) software is used to plot the obtained data. PXRD was recorded using Rigaku SmartLab X-RAY diffractometer. Time-resolved fluorescence measurements were completed using a time-correlated single photon counting (TCSPC) unit (Horiba Deltaflex).

2. Synthetic procedure and optimization

2.1. Synthesis of 10-butyl-10H-phenothiazine-3,7-dicarbaldehyde (2):



Scheme S1. Synthetic scheme for **2** in two steps.

Step-I: In a 100 ml round bottom flask, phenothiazine (5 g, 25.1 mmol) was dissolved in 30 ml DMF and followed by the slow addition of NaH (5 g, 125.5 mmol) at 0 $^{\circ}$ C. After 30 min, n-bromobutane was added slowly at 25 $^{\circ}$ C and heated the reaction at 70 $^{\circ}$ C. After 3 h, reaction was cooled down to 25 $^{\circ}$ C followed by the addition of water and product was extracted using hexane. The organic layer was washed with brine and dried over anhydrous MgSO₄ followed by the filtration and evaporation under reduced pressure to get the crude product **1** which was directly used for the next step without any purification.

Step-II: This step was adapted from previously reported literature¹ and subsequently modified. In a 100 ml 2 neck round bottom flask, 53 ml of POCl₃ (87 g, 565 mmol) was dissolved in 41 ml DMF (520 mmol) and stirred for 30 min at 0 $^{\circ}$ C followed by the slow addition of crude **1** to the reaction mixture. This reaction was heated at 100 $^{\circ}$ C. After 48 h, reaction was cooled down to 25 $^{\circ}$ C followed by the neutralization with NaOH solution by keeping in ice bath and extracted with chloroform. The chloroform layer was washed with brine and dried over anhydrous MgSO₄ followed by filtration and evaporation under reduced pressure. Product **3** was purified using 2:2

EtOAc:Petroleum ether to afford yellow colored compound (5.5 g, 70% yield).): HRMS (ESI) m/z : $[M+H]^+$ Calcd for $C_{18}H_{17}NO_2S$ 312.1053 Da (most abundant isotopologue); Found 312.1060 Da (most abundant isotopologue). 1H -NMR (300 MHz, $DMSO-d_6$, 25 °C): δ 9.81 (s, 2CHO), 7.74 (d, $J = 7.8$ Hz, 2H), 7.62 (s, 2H), 7.24 (d, $J = 8.5$ Hz, 2H), 4.00 (t, $J = 7.3$ Hz, CH_2), 1.73-1.63 (m, CH_2), 1.47-1.34 (m, CH_2), 0.87 (t, $J = 7.2$ Hz, CH_3) $^{13}C\{^1H\}$ -NMR (75.5 MHz, $DMSO-d_6$, 25 °C): δ 190.7, 148.4, 131.7, 130.2, 128.0, 123.0, 116.5, 47.2, 28.1, 19.2, 13.6.

2.2. BIZM synthesis optimization using malonic acid:

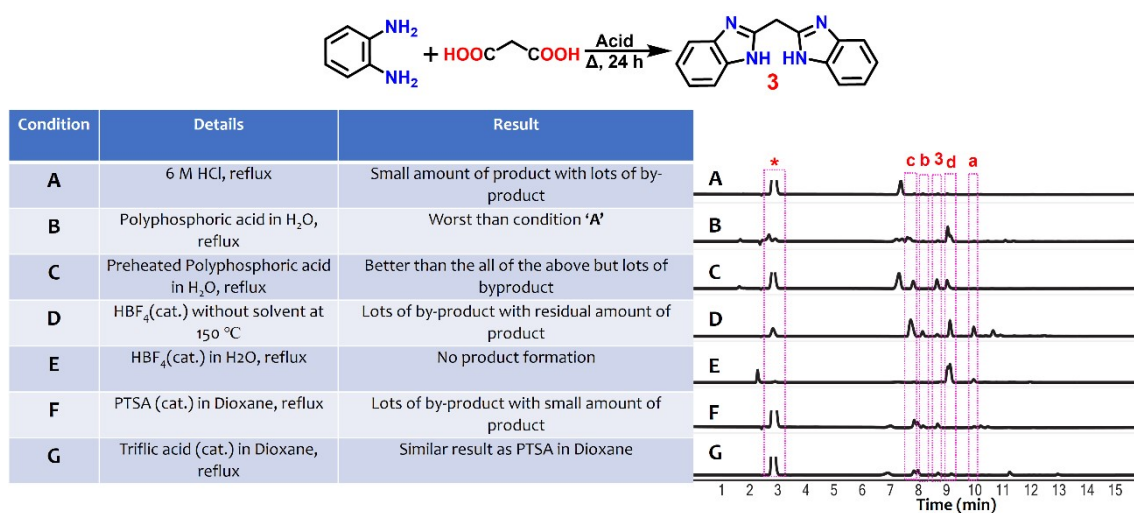


Figure S1. All optimization reactions are carried out for 24 h. Analytical RP-HPLC profile ($\lambda = 280$ nm). Reaction optimization of methylenebisbenzimidazole (BIZM) using malonic acid. '*' represent remain diaminobenzene. a, b, c, and d represent by-product formed during reaction (structure mentioned below). A linear gradient of 10%-100% of buffer B in buffer A over 10 min including 3 min equilibration using an Agilent Zorbax SB-C3, 5 μ m, 4.6 \times 150 mm, LC column with 0.9 mL/min flow rate was used for the chromatographic separation (buffer A= 0.1%TFA in water; buffer B= 0.08%TFA in acetonitrile).

2.3. BIZM synthesis optimization using malonamide:

Even after changing the malonic acid to malonamide (Figure S2i (A)) we noticed significant amount of the hydrolyzed byproduct (b) which further result in decarboxylated byproduct (c) in heating condition. This amide hydrolysis was happening in presence of water under heating condition, so we decided to change the solvent which has similar boiling point and high miscibility with water (to precipitate out the final product easily) and choose 1,4-dioxane (b.p. 101 °C) as solvent. We screened the organic acid as a catalyst in 1,4-dioxane solvent condition and noticed the remarkable improvement with *p*-toluenesulfonic acid (PTSA) (C) and triflic acid (D). After optimizing the final conditions, we choose triflic acid condition as it resulted faster and clean conversion.

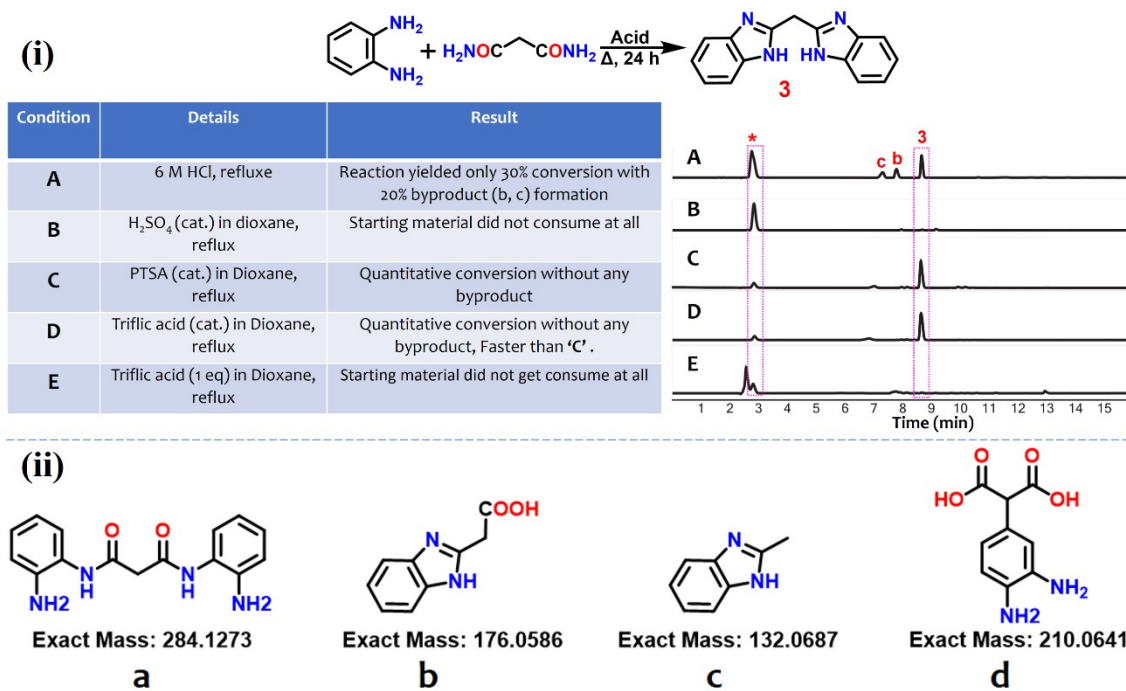


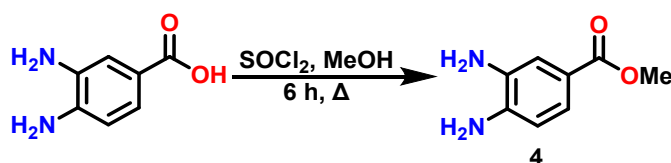
Figure S2. All optimization reactions are carried out for 24 h. (i). Analytical RP-HPLC profile ($\lambda=280$ nm). Reaction optimization of bisbenzimidazole (BIZM) using malonamide. ‘*’ represent remain diaminobenzene. b, and c represent by-product formed during reaction. A linear gradient of 10%-100% of buffer B in buffer A over 10 min including 3 min equilibration using an Agilent Zorbax SB-C3, 5 μ m, 4.6 \times 150 mm, LC column with 0.9 mL/min flow rate was used for the chromatographic separation (buffer A= 0.1%TFA in water; buffer B= 0.08%TFA in acetonitrile); (ii). Chemical structure of the by-product found during BIZM reaction optimization (predicted from the mass).

2.4. Comparison of product (3) conversion using malonic acid vs malonamide:

Substrate	Condition	Conversion (%) by HPLC
With Malonic acid	6 M HCl, reflux	10
	Polyphosphoric acid in H ₂ O, reflux	0
	Preheated Polyphosphoric acid in H ₂ O, reflux	10
	HBF ₄ (cat.) without solvent at 150 °C	5
	HBF ₄ (cat.) in H ₂ O, reflux	0
	PTSA (cat.) in Dioxane, reflux	5
	Triflic acid (cat.) in Dioxane, reflux	5
With Malonamide	6 M HCl, reflux	30
	H ₂ SO ₄ (cat.) in dioxane, reflux	0
	PTSA (cat.) in Dioxane, reflux	quantitative
	Triflic acid (cat.) in Dioxane, reflux	quantitative
	Triflic acid (1 equiv.) in Dioxane, reflux	5

Table S1. Reaction optimization of bisbenzimidazole (BIZM): The conversion % was calculated by the HPLC chromatogram. All optimization reactions are carried out for 24 h.

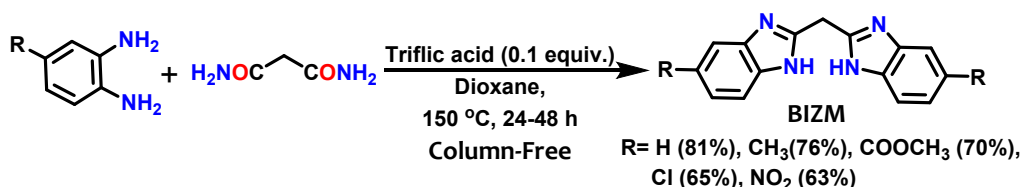
2.5. Synthesis of Methyl 3,4-diamino-benzoate (4):



Scheme S2. Synthetic scheme for 4.

Methyl 3,4-diamino-benzoate (4). To a solution of 3,4-diamino-benzoic acid (15.50 g, 100 mmol) in 150.0 ml of Methanol kept at ice-cooled bath, thionyl chloride (40 ml, 500 mmol) was added dropwise for 10 min and heated at 60 °C. After 6 h, the pH was adjusted to 8 by NaHCO_3 solution to get the precipitate. The precipitate was washed with water (2x) and dried in oven. The filtrate was partitioned between water and EtOAc to recover dissolved products (25%). The organic layer was over anhydrous magnesium sulphate followed by filtration and evaporation under reduced pressure to afford a Methyl 3,4-Diamino-benzoate 4, as a light brown solid (16.2 g, 97.0% yield, 99% HPLC purity): HRMS (ESI) m/z : $[\text{M}+\text{H}]^+$ Calcd. for $\text{C}_8\text{H}_{10}\text{N}_2\text{O}_2$ 167.0815 Da (most abundant isotopologue); Found 167.0820 Da (most abundant isotopologue). $^1\text{H-NMR}$ (300 MHz, $\text{DMSO-}d_6$, 25 °C): δ 7.16 (s, 1H), 7.10 (d, $J = 8.12$ Hz, 1H), 6.51 (d, $J = 8.12$ Hz, 1H), 5.23 (br, 2H), 4.71 (br, 2H), 3.71 (s, 3H); $^{13}\text{C}\{^1\text{H}\}\text{-NMR}$ (75.5 MHz, $\text{DMSO-}d_6$, 25 °C): δ 166.9, 140.6, 133.8, 120.4, 117.2, 114.9, 112.7, 51.1.

2.6. General procedure for BIZM and its analogue synthesis:



Scheme S3. Synthetic scheme for BIZM.

General procedure for BIZM synthesis: 4-substituted diaminobenzene (1 equiv., 1 M) and malonamide² (0.5 equiv., 0.5 M) were taken together in 1,4-dioxane, followed by the addition of triflic acid (0.1 equiv., 0.1 M) to the suspension. The reaction mixture was reflux till the completion by keeping the oil-bath temperature at 150 °C under N_2 atmosphere. The reaction mixture was concentrated to the $\frac{1}{4}$ th of solvent volume after reaction completion. Compound was precipitated by adding the 10% NaHCO_3 solution and adjustment of the pH to 8. Final precipitate was filtered and washed with water (3x) to remove the excess NaHCO_3 . The precipitation was dried in oven overnight to get the grey powder.

Bis(1H-benzo[d]imidazol-2-yl)methane (3): *o*-Phenylenediamine (32.5 g, 300 mmol), malonamide (15.75 g, 150 mmol), triflic acid (3 ml, 30 mmol) and 200 ml dioxane was taken to synthesize the **3** by following the general procedure of **Section 2.6** for 24 h to get 30.1 g of light grey powder (81.0% yield, 98% HPLC purity): HRMS (ESI) *m/z*: [M+H]⁺ Calcd for C₁₅H₁₂N₄ 249.1135 Da (most abundant isotopologue); Found 249.1159 Da (most abundant isotopologue). ¹H-NMR (300 MHz, DMSO-*d*₆, 25 °C): δ 12.45 (br, 2 NH), 7.51 (br, 4H), 7.16-7.14 (m, 4H), 4.49 (s, CH₂); ¹³C{¹H}-NMR (75.5 MHz, DMSO-*d*₆, 25 °C): δ 165.9, 150.4, 129.8, 125.0, 121.6, 29.5.

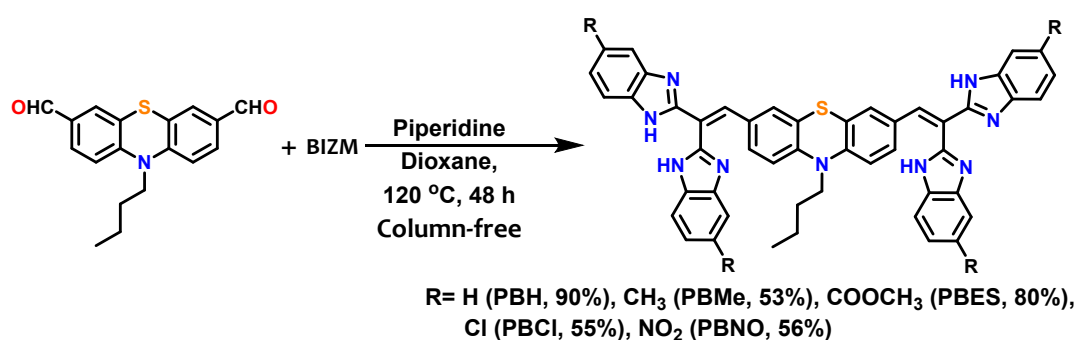
Dimethyl 2,2'-methylenebis(1H-benzo[d]imidazole-5-carboxylate) (5): Methyl 3,4-diaminobenzoate (10 g, 60.2 mmol), malonamide (3.14 g, 30.1 mmol), triflic acid (0.3 ml, 3 mmol) and 100 ml dioxane was taken to synthesize the **5** by following the general procedure of **Section 2.6** for 48 h to get 7.7 g of light pear green powder (80.0% yield, 98% HPLC purity): HRMS (ESI) *m/z*: [M+H]⁺ Calcd for C₁₉H₁₆N₄O₄ 365.1244 Da (most abundant isotopologue); Found 365.1254 Da (most abundant isotopologue). ¹H-NMR (300 MHz, DMSO-*d*₆, 25 °C): δ 8.14 (s, 2H), 7.82 (d, *J* = 8.28 Hz, 2H), 7.61 (d, *J* = 8.28 Hz, 2H), 4.61 (s, CH₂), 3.86 (s, 2CH₃); ¹³C{¹H}-NMR (75.5 MHz, DMSO-*d*₆, 25 °C): δ 166.8, 152.8, 141.9, 138.8, 123.1, 123.0, 116.9, 114.5, 52.0, 29.5.

Bis(5-methyl-1H-benzo[d]imidazol-2-yl)methane (6): 4-Methyle-*o*-phenylenediamine (1.26 g, 10 mmol), malonamide (0.52 g, 5 mmol), triflic acid (0.1 ml, 1 mmol) and 20 ml dioxane was taken to synthesize the **6** by following the general procedure of **Section 2.6** for 36 h to get 1.05 g of light grey powder (76.0% yield, 98% HPLC purity): HRMS (ESI) *m/z*: [M+H]⁺ Calcd for C₁₇H₁₆N₄ 277.1448 Da (most abundant isotopologue); Found 277.1453 Da (most abundant isotopologue). ¹H-NMR (300 MHz, DMSO-*d*₆, 25 °C): δ 7.38 (d, *J* = 7.78 Hz, 2H), 7.29 (s, 2H), 6.97 (d, *J* = 7.78 Hz, 2H), 4.42 (s, CH₂), 2.39 (s, 2CH₃); ¹³C{¹H}-NMR (75.5 MHz, DMSO-*d*₆, 25 °C): δ 149.9, 138.6, 137.4, 130.6, 122.9, 114.7, 114.1, 29.4, 21.3.

Bis(5-chloro-1H-benzo[d]imidazol-2-yl)methane (7): 4-Chloro-*o*-phenylenediamine (1.47 g, 10 mmol), malonamide (0.52 g, 5 mmol), triflic acid (0.1 ml, 1 mmol) and 20 ml dioxane was taken to synthesize the **7** by following the general procedure of **Section 2.6** for 48 h to get 1.03 g of brown powder (65.0% yield, 99% HPLC purity): HRMS (ESI) *m/z*: [M+H]⁺ Calcd for C₁₅H₁₀Cl₂N₄ 317.0355 Da (most abundant isotopologue); Found 317.0372 Da (most abundant isotopologue). ¹H-NMR (300 MHz, DMSO-*d*₆, 25 °C): δ 7.57 (s, 2H), 7.52 (d, *J* = 8.5 Hz, 2H), 7.18 (d, *J* = 8.5 Hz, 2H), 4.50 (s, CH₂); ¹³C{¹H}-NMR (75.5 MHz, DMSO-*d*₆, 25 °C): δ 151.6, 140.0, 126.0, 121.8, 115.8, 114.8, 29.4.

Bis(5-nitro-1H-benzo[d]imidazol-2-yl)methane (8): 4-Nitro-*o*-phenylenediamine (1.56 g, 10 mmol), malonamide (0.52 g, 5 mmol), triflic acid (0.1 ml, 1 mmol) and 20 ml dioxane was taken to synthesize the **8** by following the general procedure of Section 2.6 till 48 h to get 1.1 g of brown powder (63.0% yield, 92% HPLC purity): HRMS (ESI) m/z : $[M+H]^+$ Calcd for $C_{15}H_{10}N_6O_4$ 339.0836 Da (most abundant isotopologue); Found 339.0838 Da (most abundant isotopologue). 1H -NMR (300 MHz, DMSO- d_6 , 25 °C): δ 8.44 (s, 1H), 8.11 (d, J = 8.55 Hz, 2H), 7.71 (d, J = 8.55 Hz, 2H), 4.68 (s, CH_2); $^{13}C\{^1H\}$ -NMR (75.5 MHz, DMSO- d_6 , 25 °C): δ 154.8, 143.4, 142.5, 117.6, 115.6, 111.5, 29.7.

2.7. General procedure for Probe and its analogue synthesis:



Scheme S4. Synthetic scheme for the probe.

General procedure for the probe synthesis: 10-butyl-10*H*-phenothiazine- 3, 7- dicarbaldehyde (1 equiv., 0.2 M) and **BIZM** (1.1 equiv., 0.22 M) were taken together in 1,4-dioxane followed by the addition of piperidine (5 equiv., 1 M). The reaction mixture was refluxed at 120 °C (oil-bath temperature) under N₂ atmosphere for 48 h. The red colored precipitate (black for PBNO) will occur in the reaction mixture over the time which is the indication of product formation. The final red-precipitate is filtered out and washed with 1,4- dioxane (2x), EtOAc (2x), and water (2x) to remove impurity along with the piperidine. Products are lyophilized to get amorphous powder.

PBH (9): Compound **2** (0.50 g, 1.6 mmol), **3** (0.84 g, 3.31 mmol), piperidine (0.8 ml, 8.1 mmol) and 20 ml dioxane was taken to synthesize the **PBH (9)** by following the general procedure of **Section 2.7** to get 1.3 g of orange powder (90.0% yield, 91% HPLC purity): HRMS (ESI) m/z : $[M+H]^+$ Calcd for $C_{48}H_{37}N_9S$ 772.2965 Da (most abundant isotopologue); Found 772.3013 Da (most abundant isotopologue). 1H -NMR (300 MHz, DMSO- d_6 , 25 °C): δ 12.68 (s, 2NH), 12.27 (s, 2NH), 7.91 (s, 2H), 7.72 (br, 2H), 7.57-7.54 (m, 4H), 7.43 (br, 3H), 7.30 (br, 3H), 7.16 (br, 6H), 6.82 (br, 4H), 3.74 (t, J = 5.55 Hz, CH_2), 1.57-1.47 (m, CH_2), 1.36-1.24 (m, CH_2), 0.81 (t, J = 7.04 Hz, CH_3); $^{13}C\{^1H\}$ -NMR (75.5 MHz, DMSO- d_6 , 25 °C): δ 151.6, 149.8, 147.9, 144.1, 143.6,

134.8, 134.7, 134.5, 129.4, 128.9, 127.9, 122.7 122.5, 122.2, 121.7, 121.5, 120.5, 119.3, 118.6, 115.7, 111.7, 111.4, 46.2, 28.2, 19.2, 13.6.

PBES (10): Compound **2** (0.1 g, 0.32 mmol), **5** (0.27 g, 0.67 mmol), piperidine (0.15 ml, 1.6 mmol) and 10 ml dioxane was taken to synthesize the **PBES (10)** by following the general procedure of **Section 2.7** to get 0.26 g of brown powder (80.0% yield, 98% HPLC purity): HRMS (ESI) m/z : $[M+H]^+$ Calcd for $C_{56}H_{45}N_9O_8S$ 1004.3185 Da (most abundant isotopologue); Found 1004.3190 Da (most abundant isotopologue). 1H -NMR (300 MHz, $DMSO-d_6$, 25 °C): δ 13.13 (s, 2NH), 12.70-12.64 (m, 2NH), 8.35 (s, 1H), 8.18-8.14 (m, 2H), 8.04-7.94 (m, 5H), 7.82 (br, 3H), 7.66 (br, 2H), 7.54 (br, 1H), 6.84 (br, 6H), 3.92 (s, 2CH₃), 3.85 (s, 2CH₃), 3.79 (m, CH₂), 1.50 (br, CH₂), 1.28-1.24 (m, CH₂), 0.81-0.79 (m, CH₃); $^{13}C\{^1H\}$ -NMR (75.5 MHz, $DMSO-d_6$, 25 °C): δ 166.8 (not well resolved), 154.3, 153.5, 150.2, 149.9, 147.0, 144.4, 143.2, 138.3, 136.8, 134.5, 129.0, 128.2, 124.0, 123.5, 122.1, 121.0, 120.3, 119.4, 118.4, 115.8, 113.5, 111.8, 52.1, 52.0, 46.3, 28.2, 19.2, 13.6.

PBMe (11): Compound **2** (0.1 g, 0.32 mmol), **6** (0.2 g, 0.71 mmol), piperidine (0.15 ml, 1.6 mmol) and 10 ml dioxane was taken to synthesize the **PBMe (11)** by following the general procedure of **Section 2.7** to get 0.14 g of dark red powder (53.0% yield, 98% HPLC purity): HRMS (ESI) m/z : $[M+H]^+$ Calcd for $C_{52}H_{45}N_9S$ 828.3591 Da (most abundant isotopologue); Found 828.3671 Da (most abundant isotopologue). 1H -NMR (300 MHz, $DMSO-d_6$, 25 °C): δ 12.51 (s, 2NH), 12.12 (s, 2NH), 7.84 (s, 2H), 7.53-7.23 (m, 8H), 7.10 (d, $J = 7.29$ Hz, 2H), 6.99 (d, $J = 7.29$ Hz, 2H), 6.83-6.79 (m, 6H), 3.73 (br, CH₂), 2.47 (s, 2CH₃), 2.39 (s, 2CH₃), 1.51 (br, CH₂), 1.30-1.24 (m, CH₂), 0.80 (t, $J = 6.92$ Hz, CH₃); $^{13}C\{^1H\}$ -NMR (75.5 MHz, $DMSO-d_6$, 25 °C): δ 151.3, 144.1, 134.1, 131.9, 129.5, 128.8, 128.0, 123.4, 122.2, 120.7, 118.7, 115.7 111.2, 46.2, 28.3, 21.4, 19.2, 13.6 (The quaternary carbon signals appear weak).

PBCl (12): Compound **2** (0.1 g, 0.32 mmol), **7** (0.23 g, 0.71 mmol), piperidine (0.15 ml, 1.6 mmol) and 10 ml dioxane was taken to synthesize the **PBCl (12)** by following the general procedure of **Section 2.7** to get 0.16 g of brick red powder (55.0% yield, 98% HPLC purity): HRMS (ESI) m/z : $[M+H]^+$ Calcd for $C_{48}H_{33}Cl_4N_9S$ 910.1386 Da (most abundant isotopologue); Found 910.1464 Da (most abundant isotopologue). 1H -NMR (300 MHz, $DMSO-d_6$, 25 °C): δ 12.92 (s, 2NH), 12.45 (s, 2NH), 7.93 (s, 2H), 7.79-7.73 (m, 2H), 7.64-7.60 (m, 4H), 7.46 (br, 2H), 7.32 (d, $J = 8.04$ Hz, 2H), 7.20 (d, $J = 8.04$ Hz, 2H), 6.81 (br, 6H), 3.75 (br, CH₂), 1.52 (br, CH₂), 1.30-1.23 (m, CH₂), 0.81 (t, $J = 8.0$ Hz, CH₃); $^{13}C\{^1H\}$ -NMR (75.5 MHz, $DMSO-d_6$, 25 °C): δ

152.9, 148.9, 144.3, 142.4, 135.8, 135.2, 129.1, 128.0, 126.1, 122.7, 122.2, 119.6, 118.7, 118.0, 115.8, 113.1, 111.4, 111.1, 46.3, 28.2, 19.2, 13.6 (A few quaternary carbon signals appear weak).

PBNO (13): Compound **2** (0.1 g, 0.32 mmol), **8** (0.25 g, 0.67 mmol), piperidine (0.15 ml, 1.6 mmol) and 10 ml dioxane was taken to synthesize the **PBNO (13)** by following the general procedure of **Section 2.7** to get 0.17 g of black powder (56.0% yield, 90% HPLC purity): HRMS (ESI) m/z : $[M+H]^+$ Calcd for $C_{48}H_{33}N_{13}O_8S$ 952.2369 Da (most abundant isotopologue); Found 952.2434 Da (most abundant isotopologue). 1H -NMR (300 MHz, $DMSO-d_6$, 25 °C): δ 8.57 (s, 2H), 8.40 (s, 2H), 8.22 (d, $J = 8.18$ Hz, 2H), 8.12-8.08 (m, 4H), 7.82 (d, $J = 8.18$ Hz, 2H), 7.69 (d, $J = 8.52$ Hz, 2H), 6.85 (br, 6H), 3.74 (br, CH_2), 1.51 (br, CH_2), 1.29-1.27 (m, CH_2), 0.80 (t, $J = 6.96$ Hz, CH_3); $^{13}C\{^1H\}$ -NMR (75.5 MHz, $DMSO-d_6$, 25 °C): δ 155.7, 152.2, 144.6, 142.9, 142.8, 138.0, 129.4, 128.7, 128.4, 122.1, 118.5, 118.2, 115.9, 46.4, 28.1, 19.2, 13.6 (Some of the carbon signal are very weak due to the poor solubility).

3. Spectroscopic study

Preparation of solutions:

The stock solution of probes (10^{-3} M) was prepared in DMSO. The 10^{-3} M stock solution for all the amines was prepared in DMSO.

Absorption and FL studies for solution state:

Absorption studies were carried out with the sample (2 mL, 10 μ M) in a quartz cuvette (1 cm \times 1 cm). The wavelength range was kept within 750 to 200 nm. Emission spectra of the same sample are instantaneously recorded with the range from 450 to 800 nm, with a PMT voltage of 400 eV and excitation slit/emission slit 5.0. All measurements were performed at 22 °C.

Study of probes coated films for visual detection of BAs and concentration-based changes:

For the thin film study, a 10^{-2} M solution of the **probe** was diluted with 1,4-dioxane to make 10^{-3} M and was drop-casted on glass coverslips and dried at room temperature. The dried glass coverslips were affixed on the wall of a 200 mL glass bottle sealed with a septum. For screening, 20 μ L of BAs were added, and kept in the dark at 25 °C for 4 h to get the maximum change in the observed fluorescence colour. For the variable concentration-based change, different volume (mentioned in the corresponding images) of Putrescine or Cadaverine were added, and kept in the dark at 25 °C for 2 h to get the maximum change for the particular volume of BAs. All measurements were performed at 22 °C. All the images were taken with a OnePlus Nord AC2001 (f/1.8, 1/20, ISO1600).

Absolute Quantum Yield Measurement:

The solid-state absolute quantum yield measurement used a calibrated integrating sphere method with an absolute error of $\pm 2\%$.

Time-Resolved Decay Measurement:

Solid-state lifetime measurement: The solid-state lifetime was measured for PBES thin-film (drop-casted on glass slide) treated for 2 h with putrescine vapor 0.5 μL to get PBES-R and 25 μL to get PBES-Y in 200 ml sealed flask at 25 $^{\circ}\text{C}$ in dark. The pulse diode laser used was 450 nm, with a setup target of 10000 counts. The instrument response function was measured before fluorescence lifetime measurements using water in quartz cuvette (1 cm \times 1 cm). All of the decay curves were fitted using the supplied EZ Time software. All measurements were performed at 22 $^{\circ}\text{C}$. A magic angle (54.71) configuration was used for all measurements. All fittings were done by keeping the χ^2 value around 1.

NMR Measurement:

All the compounds (15-20 mg) were dissolved in dry DMSO-d6 followed by data acquisition using 300 MHz SB (Bruker) Avance-III HD instruments.

Dynamic light scattering (DLS) Measurement:

The average particle size of the aggregated state was found using a Malvern particle size analyser (zeta sizer nano-ZS), keeping a concentration of 10 mM.

Computational Details:

Geometry optimizations of all the compounds are carried out with the aid of Density functional theory (DFT) using CAM-B3LYP exchange-correlation functional and 6-31G (d, p) basis set as implemented in Gaussian 09 suite of programs.³

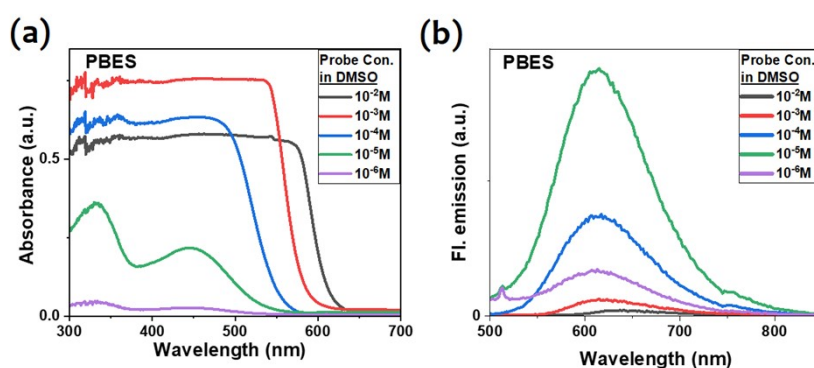


Figure S3. Absorption and emission spectra ($\lambda_{\text{ex}} = 445 \text{ nm}$) of PBES (a, b) at different concentration in DMSO.

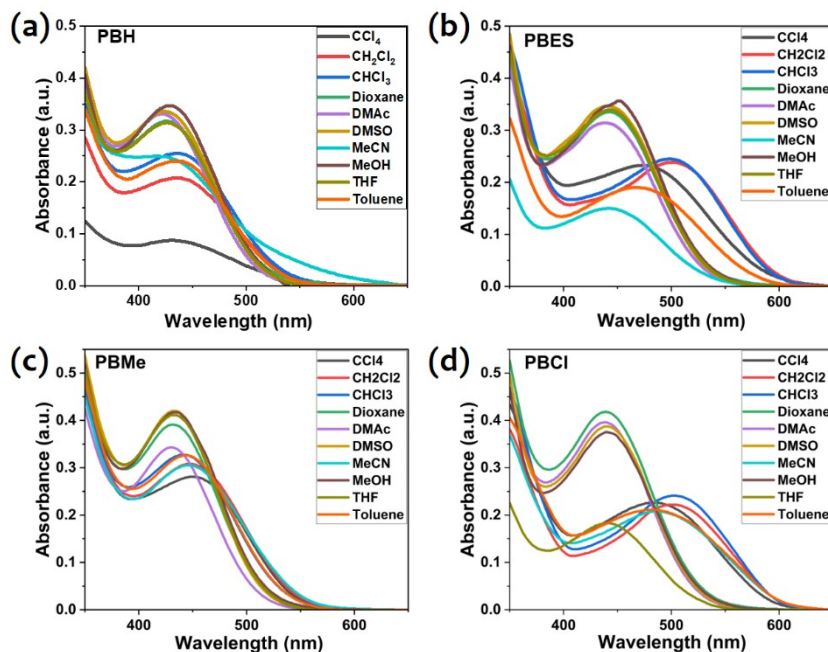


Figure S4. Absorption spectra of solvatochromic study of compounds ($10\mu\text{M}$) in different solvents: (a) **PBH**, (b) **PBES**, (c) **PBMe**, and (d) **PBCl**.

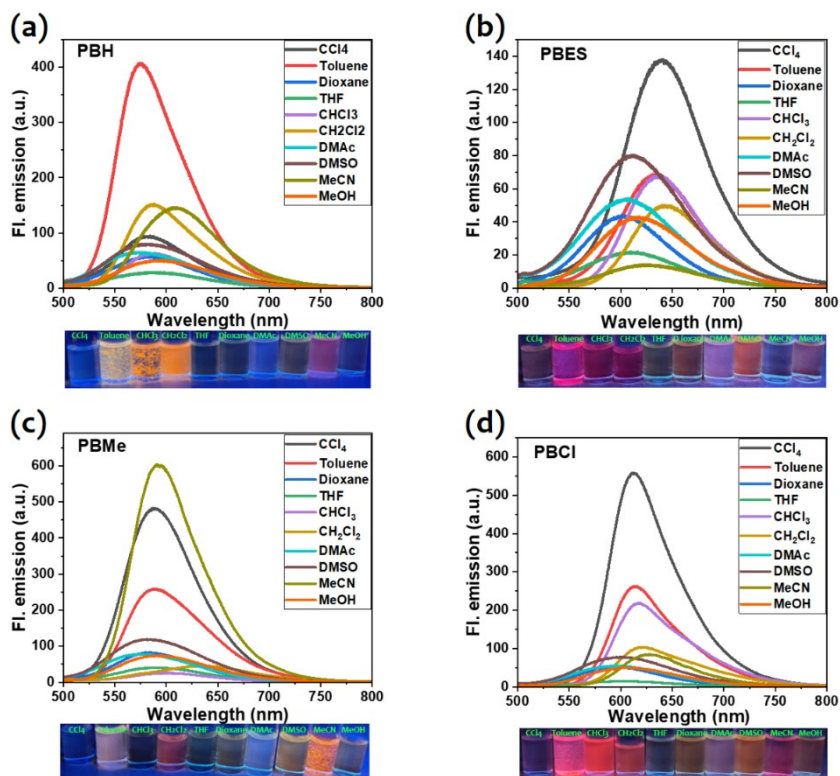


Figure S5. Emission spectra of solvatochromic study of compounds ($10\mu\text{M}$) in different solvents: (a) **PBH**, (b) **PBES**, (c) **PBMe**, and (d) **PBCl**. Excitation wavelength was chosen based on the absorption maxima.

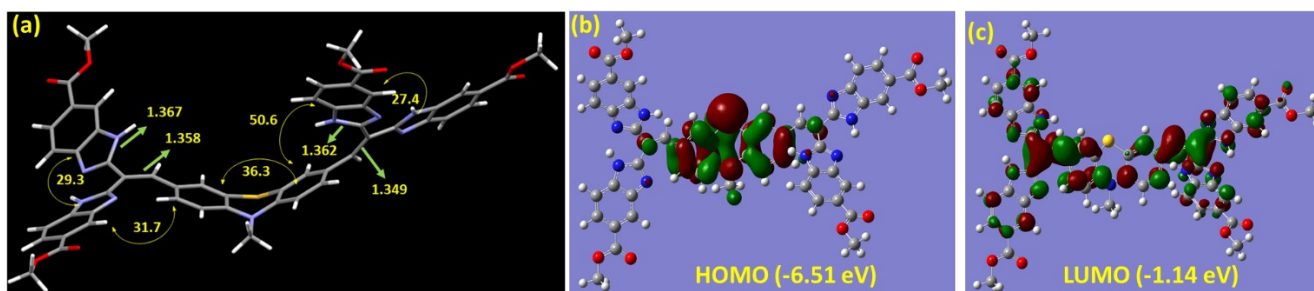


Figure S6. The DFT optimized PBES in DMSO (The *N*-alkyl chain is shortened to reduce the calculation times and there will be no change in the electronic contribution) (c) molecular geometry (conformationally twisted with selected bond length (Å) and torsion angles (°)), (b) HOMO and (c) LUMO. (See the details later).

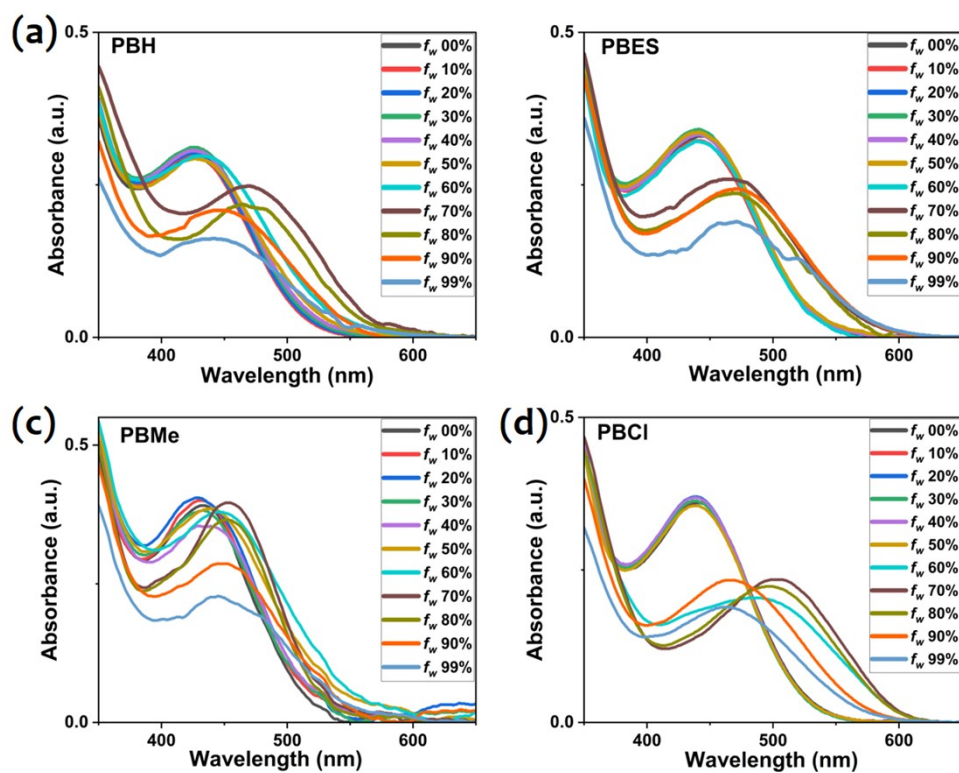


Figure S7. Absorption spectra of AIE study of compounds (10 μ M) with different fractions of water in THF: (a) PBH, (c) PBMe, (d) PBCl, and (b) PBES (water in MeCN).

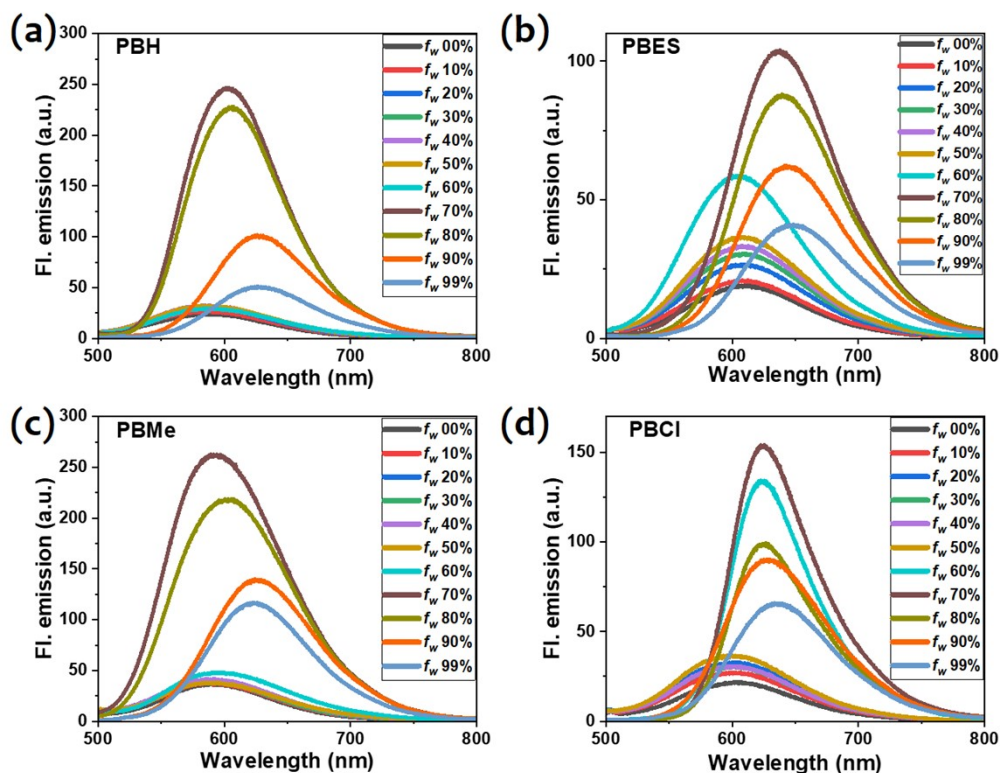


Figure S8. Emission spectra of AIE study of compounds (10 μ M) with different fractions of water in THF: (a) PBH, (c) PBMe, (d) PBCl, and (b) PBES (water in MeCN). Excitation wavelength was chosen based on the absorption maxima.

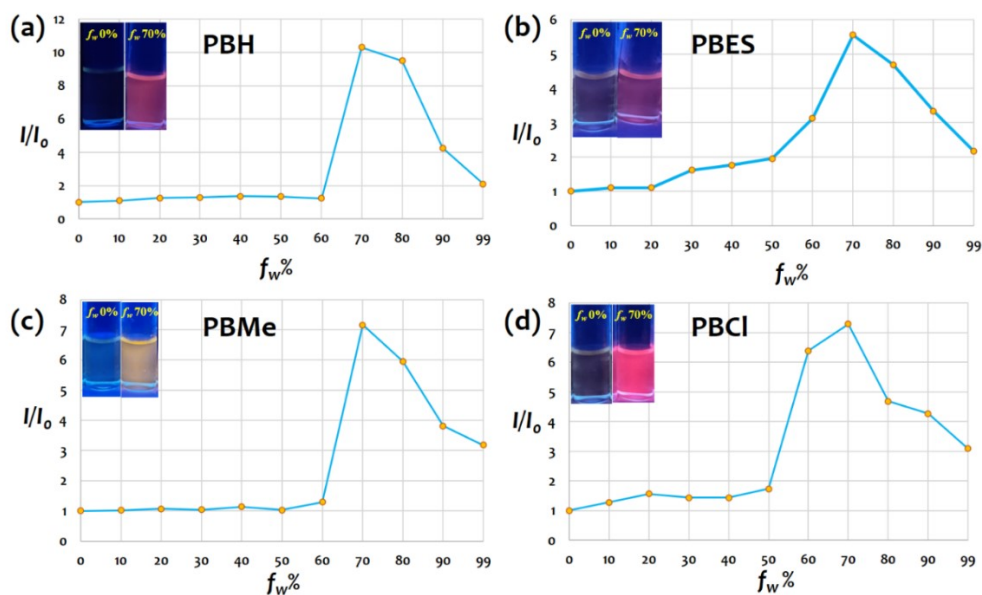


Figure S9. The I/I_0 plot (I_0 : FL intensity before addition of water, and I : FL intensity after addition of water) [probe concentration: 10 μ M] of (a) PBH; (b) PBES; (c) PBMe; and (d) PBCl. The image is taken at $f_w = 0\%$ and $f_w = 70\%$ for PBH, PBES, PBMe and PBCl under 365 nm UV lamp.

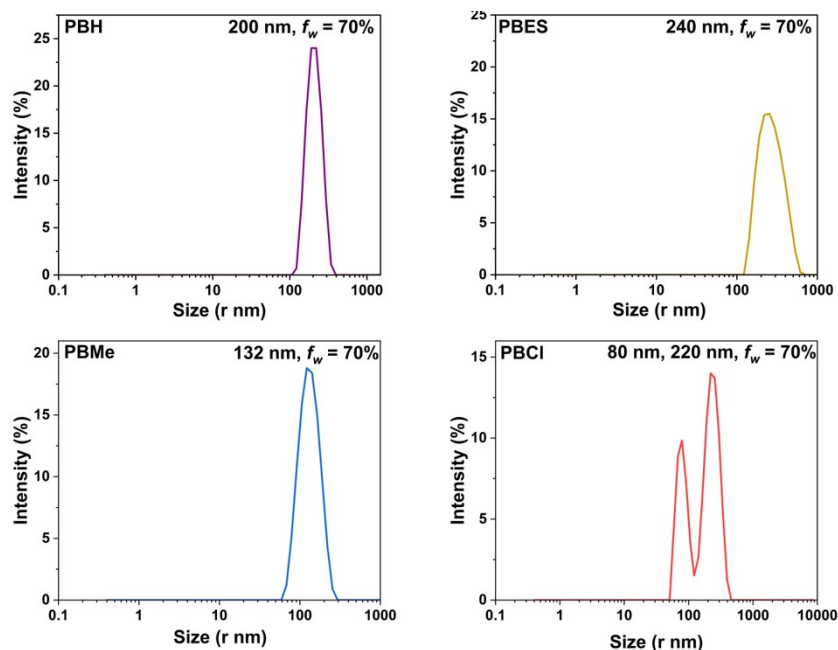


Figure S10. DLS study of the compounds for the most emissive aggregated state.

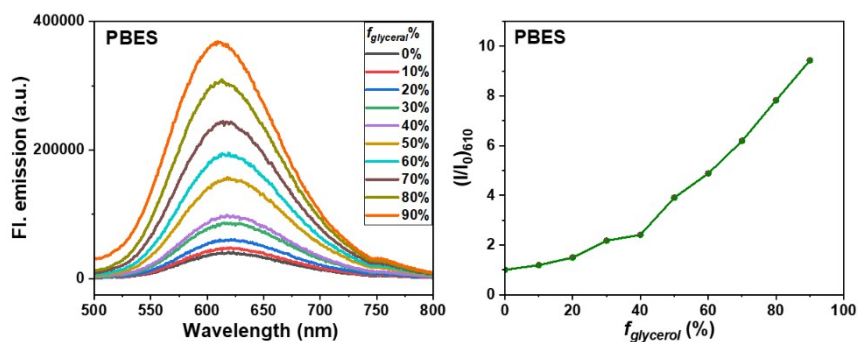


Figure S11. Compound PBES (10 μM) with different fractions of glycerol in MeOH showing viscochromism ($\lambda_{\text{ex}} = 450 \text{ nm}$).

Compound	λ_{ex}	λ_{em}
• PBH	465	612
• PBMe	481	653
• PBES	513	667
• PBCl	523	671
• PBNO	553	NE

Table S2. Solid state fluorescent spectral details of all four probes (recorded with solid powder).

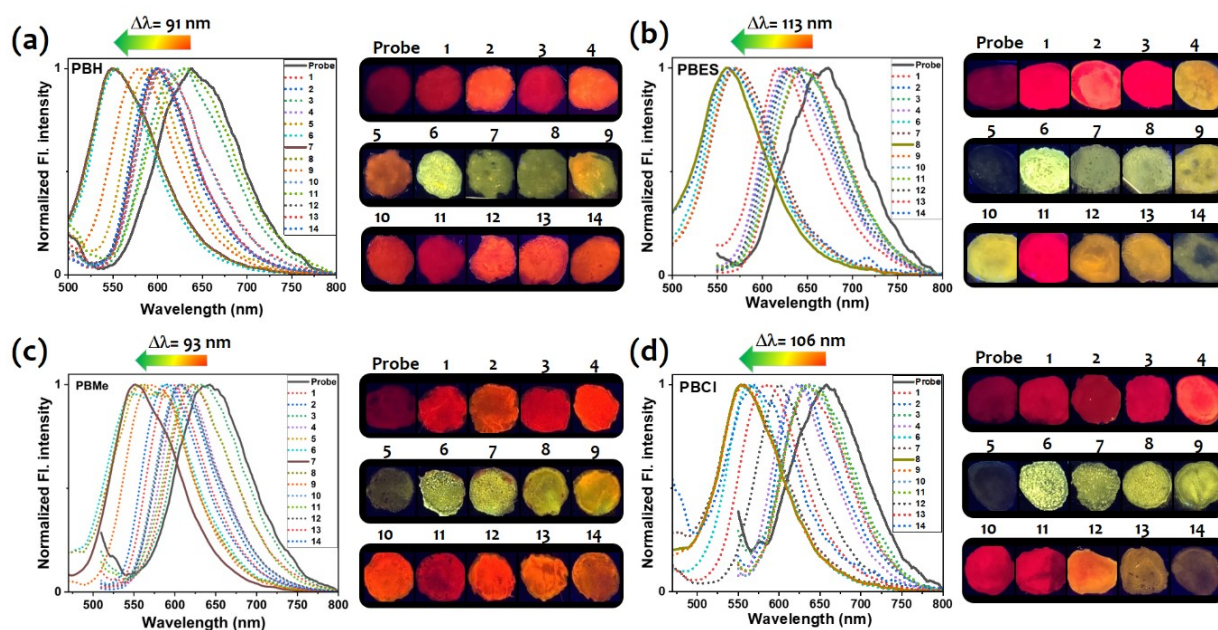


Figure S12. Solid state emission spectra of probe thin-film (drop-casted on glass slide) treated with 20 μL of different amines and biogenic amines (BAs) vapor in 200 ml sealed flask for 4 h along with their visual representation of emissive state (under 365 nm): (a) **PBH**, (b) **PBES**, (c) **PBMe**, and (d) **PBCl**. 1. Ammonia; 2. N-butylamine; 3. N, N-diisopropylethylamine; 4. 2-phenylethylamine; 5. 1,2-ethylenediamine; 6. 1,3-propanediamine; 7. 1,4-butanediamine (Putrescine); 8. 1,5-pentanediamine (Cadaverine); 9. 1,6-hexanediamine; 10. Spermidine; 11. Spermine; 12. 3-aminopropanol; 13. 4-aminobutanol; 14. N, N-dimethylaminopropylamine.

	λ_{ex}	λ_{em}	$\Delta\lambda$	QY	Absolute error	Relative error			λ_{ex}	λ_{em}	$\Delta\lambda$	QY	Absolute error	Relative error
PBH	465	638		0.42	0.084	0.1993		PBES	513	671		0.09	0.039	0.45305
1	465	605	33	0.3	0.095	0.3131		1	513	645	26	0.59	0.033	0.05593
2	465	601	37	0.48	0.103	0.2135		2	513	632	39	1.06	0.054	0.05056
3	465	629	9	0.34	0.129	0.3805		3	513	647	24	0.39	0.044	0.11456
4	465	601	37	0.59	0.086	0.147		4	513	629	42	1.75	0.099	0.05677
5	465	592	46	0.53	0.074	0.1404		5	513	NA	NA	0.03	0.1411	5.18362
6	437	553	85	2.86	0.174	0.0611		6	437	568	103	4.45	0.148	0.03316
7	437	547	91	2.37	0.135	0.0571		7	437	570	101	1.08	0.112	0.10385
8	437	551	87	1.98	0.124	0.0624		8	437	558	113	1.93	0.157	0.08125
9	437	577	61	2.99	0.157	0.0526		9	437	584	87	1.5	0.088	0.05888
10	465	607	31	0.56	0.091	0.1616		10	513	641	30	7.89	0.196	0.02486
11	465	632	6	0.24	0.041	0.1725		11	513	643	28	0.78	0.037	0.04741
12	465	599	39	0.57	0.047	0.0839		12	513	634	37	0.94	0.107	0.1136
13	465	600	38	0.67	0.056	0.8323		13	513	620	51	1.05	0.149	0.14149
14	465	597	41	0.36	0.074	0.206		14	437	568	103	0.79	0.154	0.19508
	λ_{ex}	λ_{em}	$\Delta\lambda$	QY	Absolute error	Relative error			λ_{ex}	λ_{em}	$\Delta\lambda$	QY	Absolute error	Relative error
PBMe	481	642		0.46	0.066	0.1426		PBCI	523	659		0.17	0.065	0.38707
1	481	623	19	1.02	0.052	0.051		1	523	636	23	0.73	0.054	0.07425
2	481	606	36	1.35	0.051	0.0379		2	523	624	35	1.2	0.079	0.06577
3	481	633	9	0.57	0.046	0.0805		3	523	641	18	0.44	0.062	0.13929
4	481	612	30	1.41	0.077	0.0545		4	523	620	39	1.22	0.047	0.03811
5	437	572	70	1.26	0.29	0.2294		5	437	550	109	0.74	0.17	0.2313
6	437	548	94	1.59	0.069	0.0435		6	437	555	104	2.43	0.173	0.0719
7	437	549	93	2.57	0.165	0.0642		7	437	557	102	1.98	0.16	0.08069
8	437	560	82	3.12	0.201	0.0652		8	437	553	106	2	0.122	0.06133
9	437	569	73	2.43	0.118	0.0486		9	437	557	102	2.02	0.164	0.08088
10	481	607	35	1.3	0.048	0.0374		10	523	634	25	0.57	0.072	0.12681
11	481	620	22	0.85	0.052	0.0615		11	523	633	26	0.58	0.053	0.0923
12	481	607	35	1.29	0.061	0.0473		12	437	600	59	1.2	0.103	0.08612
13	481	598	44	1.34	0.057	0.0428		13	437	583	76	1.26	0.144	0.11491
14	481	592	50	1.97	0.06	0.0306		14	437	570	89	2	0.206	0.10343

Table S3. QY (%) and spectral details of all four probes related to Figure S11:

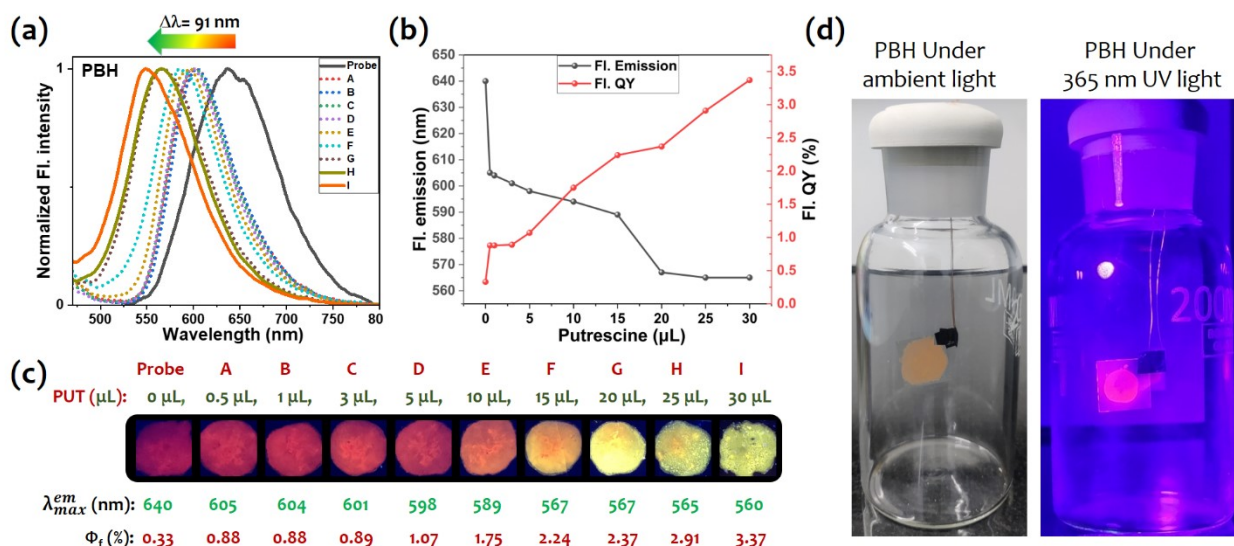


Figure S13. (a) Emission spectra of PBH thin-film (drop-casted on glass slide) treated with different amount of putrescine (PUT) in 200 ml sealed flask for 2 h; (b) Plot between wavelength emission maxima and QY vs concentration of putrescine; (c) Visual image of PBH under 365 nm UV lamp; (d) Probe drop casted on glass cover-slip complete setup for amine vapor treatment.

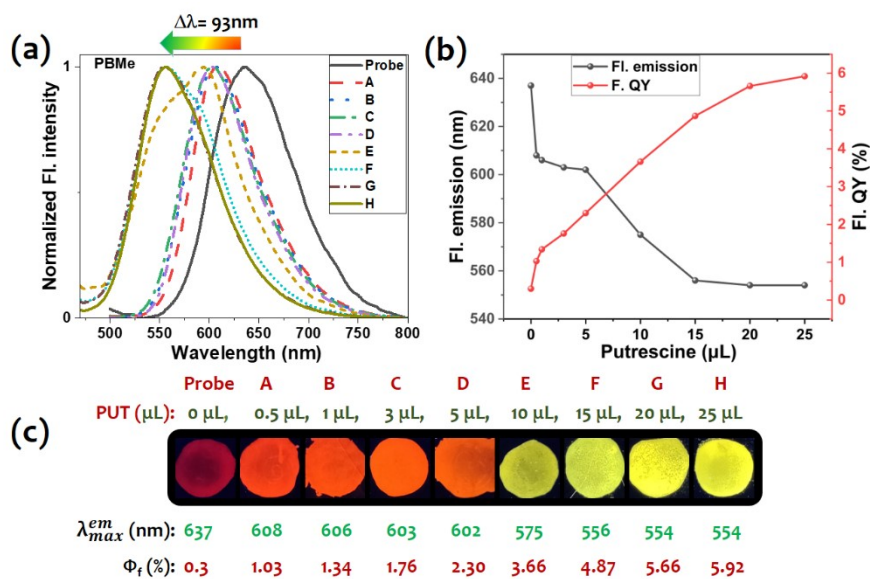


Figure S14. (a) Emission spectra of PBMe thin-film (drop-casted on glass slide) treated with different amount of PUT in 200 ml sealed flask for 2 h; (b) Plot between wavelength emission maxima and QY vs concentration of PUT; (c) Visual image of PBMe under 365 nm UV lamp.

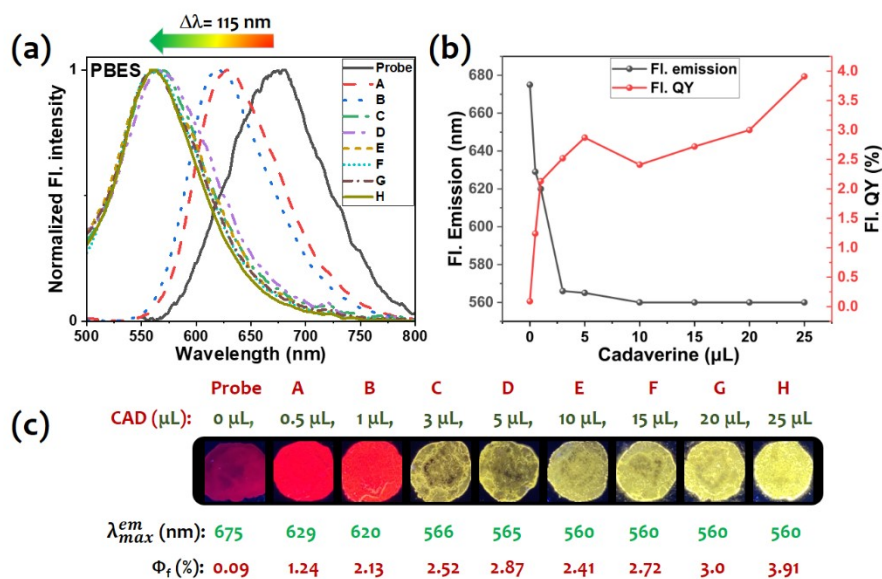


Figure S15. (a) Emission spectra of **PBES** thin-film (drop-casted on glass slide) treated with different amount of cadaverine (**CAD**) in 200 ml sealed flask for 2 h; (b) Plot between wavelength emission maxima and QY vs concentration of putrescine; (c) Visual image of **PBES** under 365 nm UV lamp.

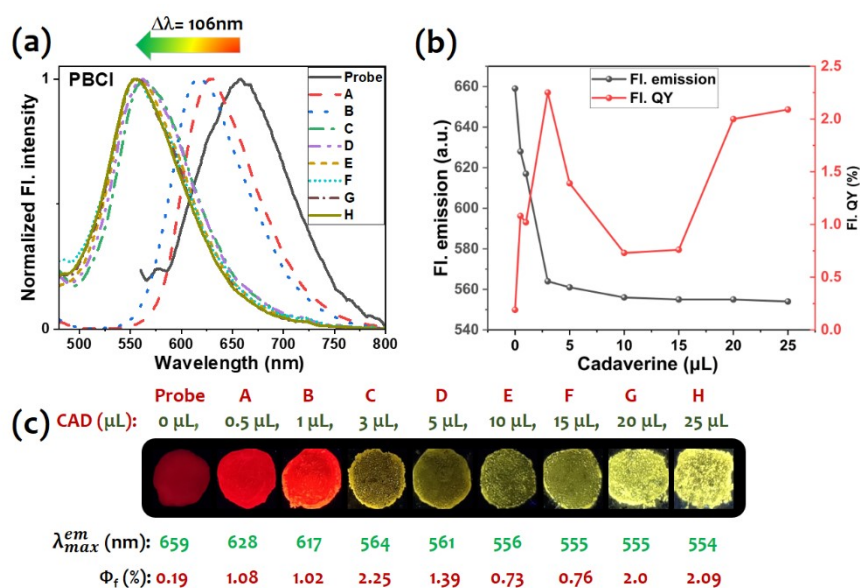


Figure S16. (a) Emission spectra of **PBCl** thin-film (drop-casted on glass slide) treated with different amount of **PUT** in 200 ml sealed flask for 2 h; (b) Plot between wavelength emission maxima and QY vs concentration of **PUT**; (c) Visual image of **PBCl** under 365 nm UV lamp.

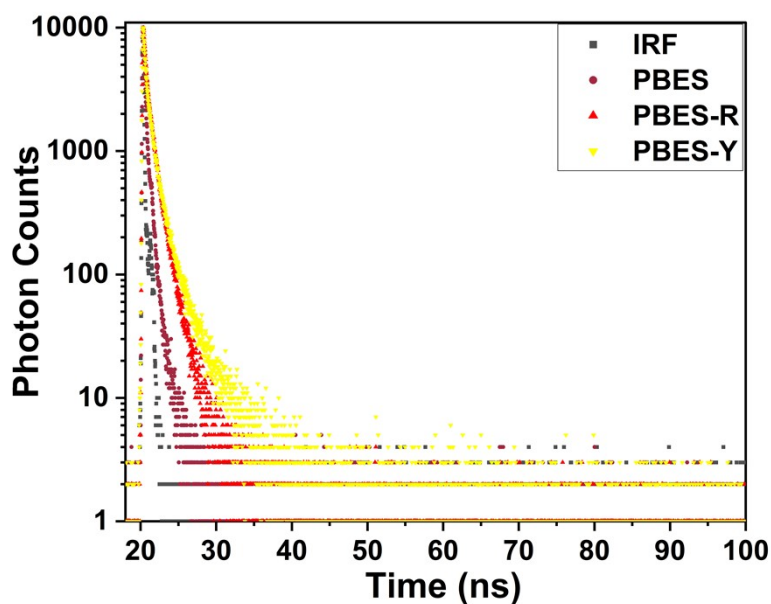


Figure S17. Lifetime decay plot for PBES, PBES-R, and PBES-Y.

(a)

Samples	α_1	α_2	α_3	τ_1	τ_2	τ_3	$\langle \tau \rangle$	χ^2
PBES	0.16	0.83	0.01	0.19	0.39	0.78	0.07	1.33
PBES-R	0.17	0.04	0.79	0.4	0.81	1.62	0.14	1.2
PBES-Y	0.22	0.04	0.74	0.48	0.95	1.9	0.18	1.12

(b)

Samples	QY	$\langle \tau \rangle$	k_r	k_{nr}
PBES	0.0009	0.07	0.01	14.27
PBES-R	0.0124	0.14	0.09	7.05
PBES-Y	0.0391	0.18	0.22	5.34

Table S4. (a) Parameter related to a lifetime (ns) measurement of the excited state. $\lambda_{ex} = 450$ nm; (b) Values calculated for radiative (ns^{-1}) and non-radiative rate constant (ns^{-1}).

Where radiative rate constant (k_r) = $\frac{QY}{\langle \tau \rangle}$ and non-radiative rate constant (k_{nr}) = $\frac{1 - QY}{\langle \tau \rangle}$.

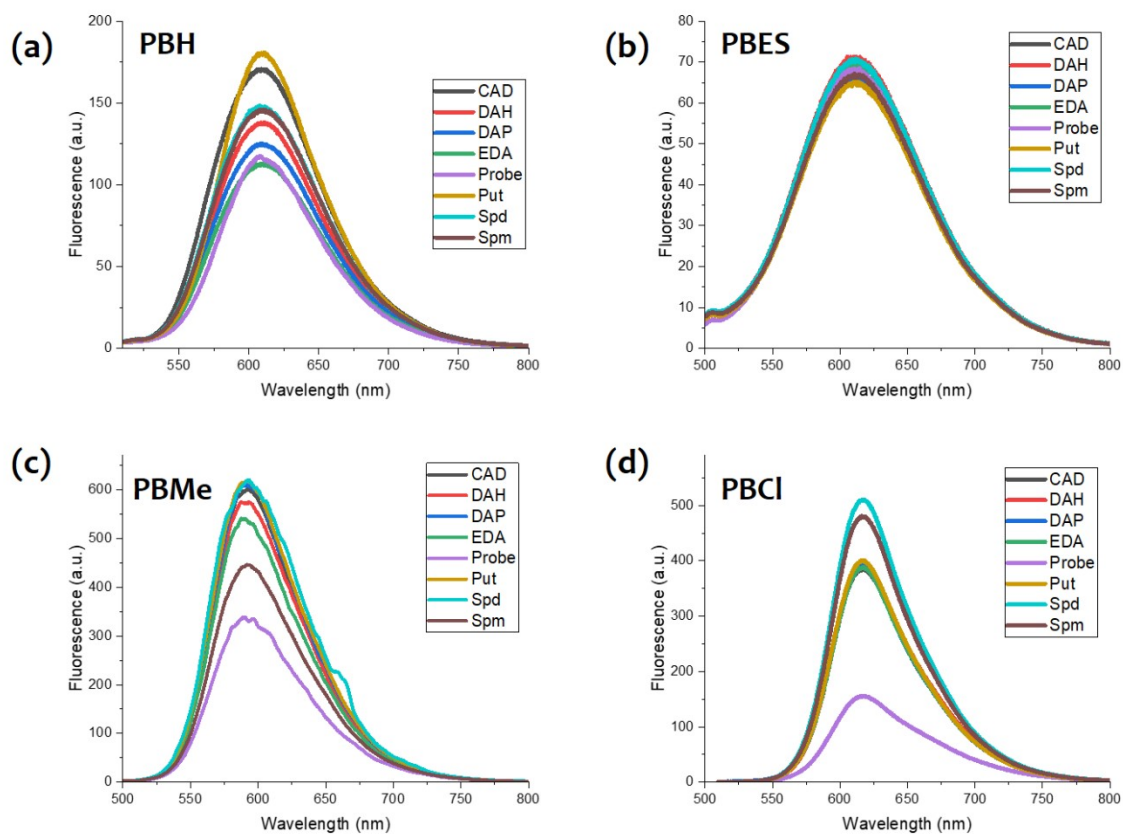


Figure S18. Solution state emission spectra for the probes (10^{-5} M) treated with BAs (10^{-5} M) in DMSO.

4. NMR and LCMS analysis for the reaction mechanism

4.1. $^1\text{H-NMR}$ study for PBES, PBES-R and PBES-Y:

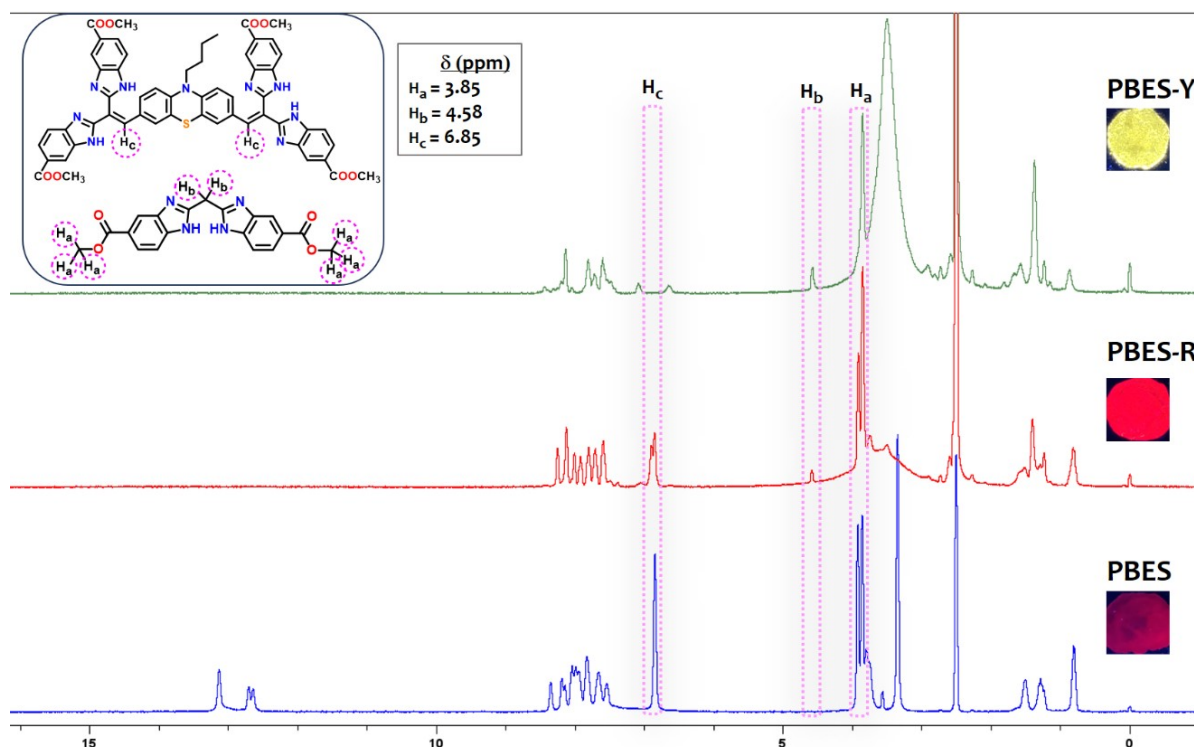


Figure S19. A complete ^1H NMR spectra of **PBES**, **PBES-R** (intermediate state of putrescine vapor exposed **PBES**), and **PBES-Y** (final state of putrescine vapor exposed **PBES**).

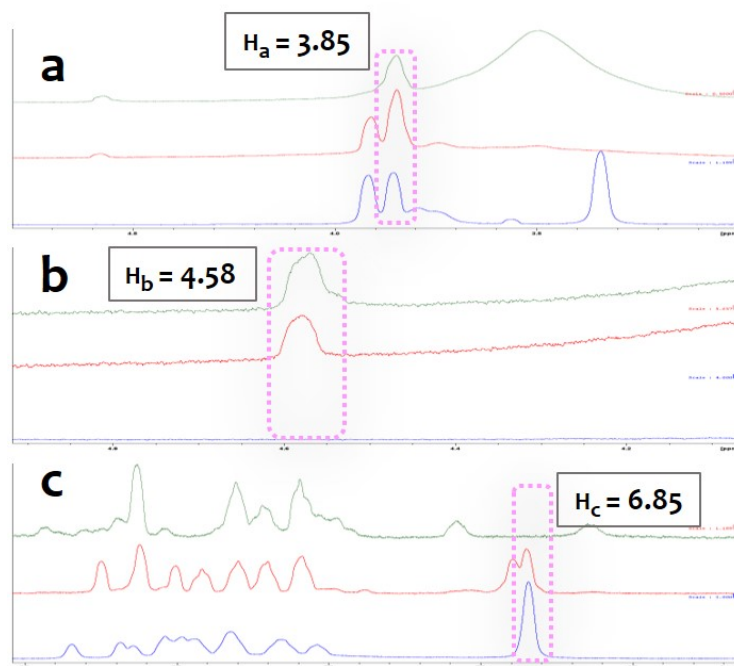
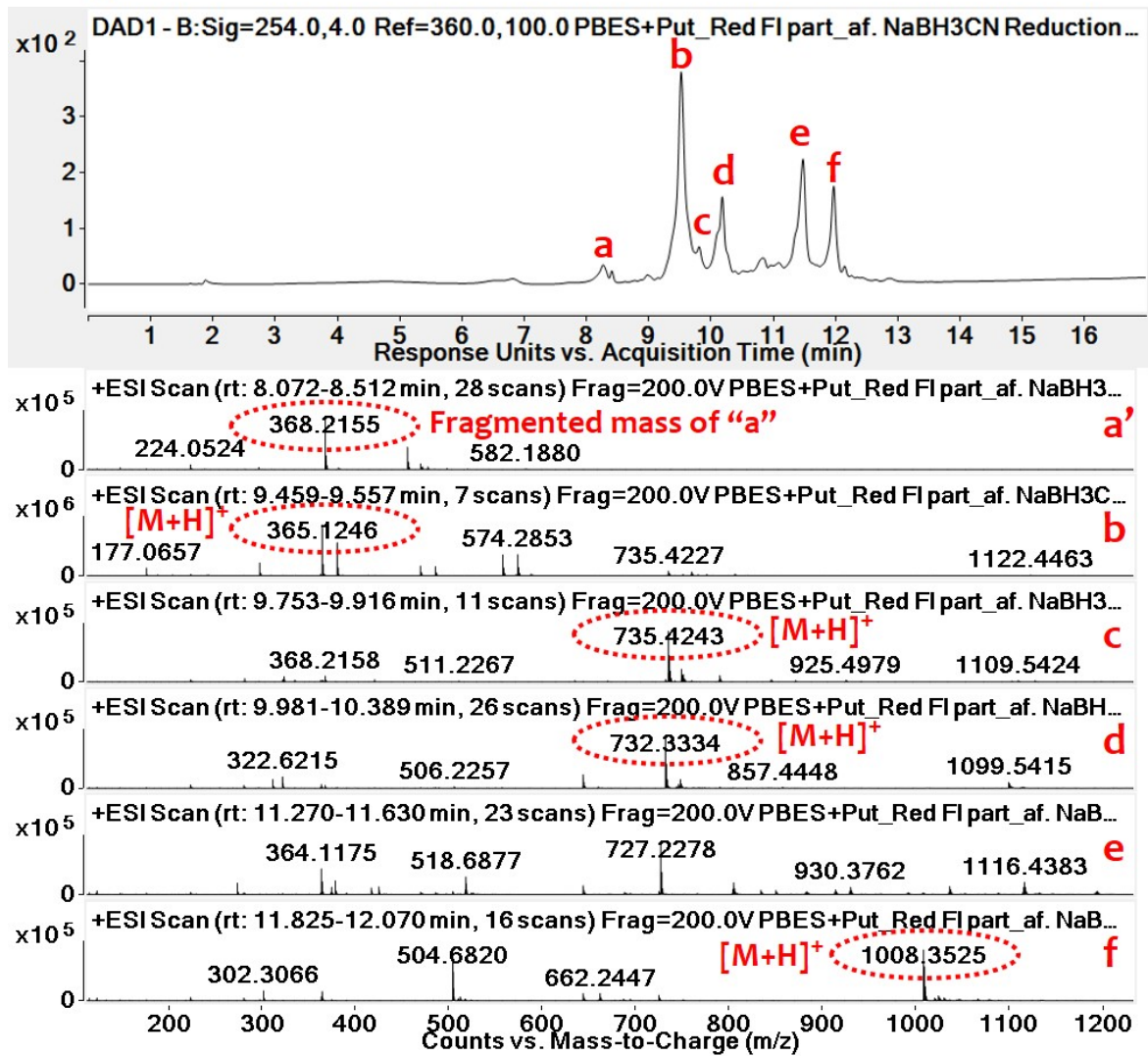


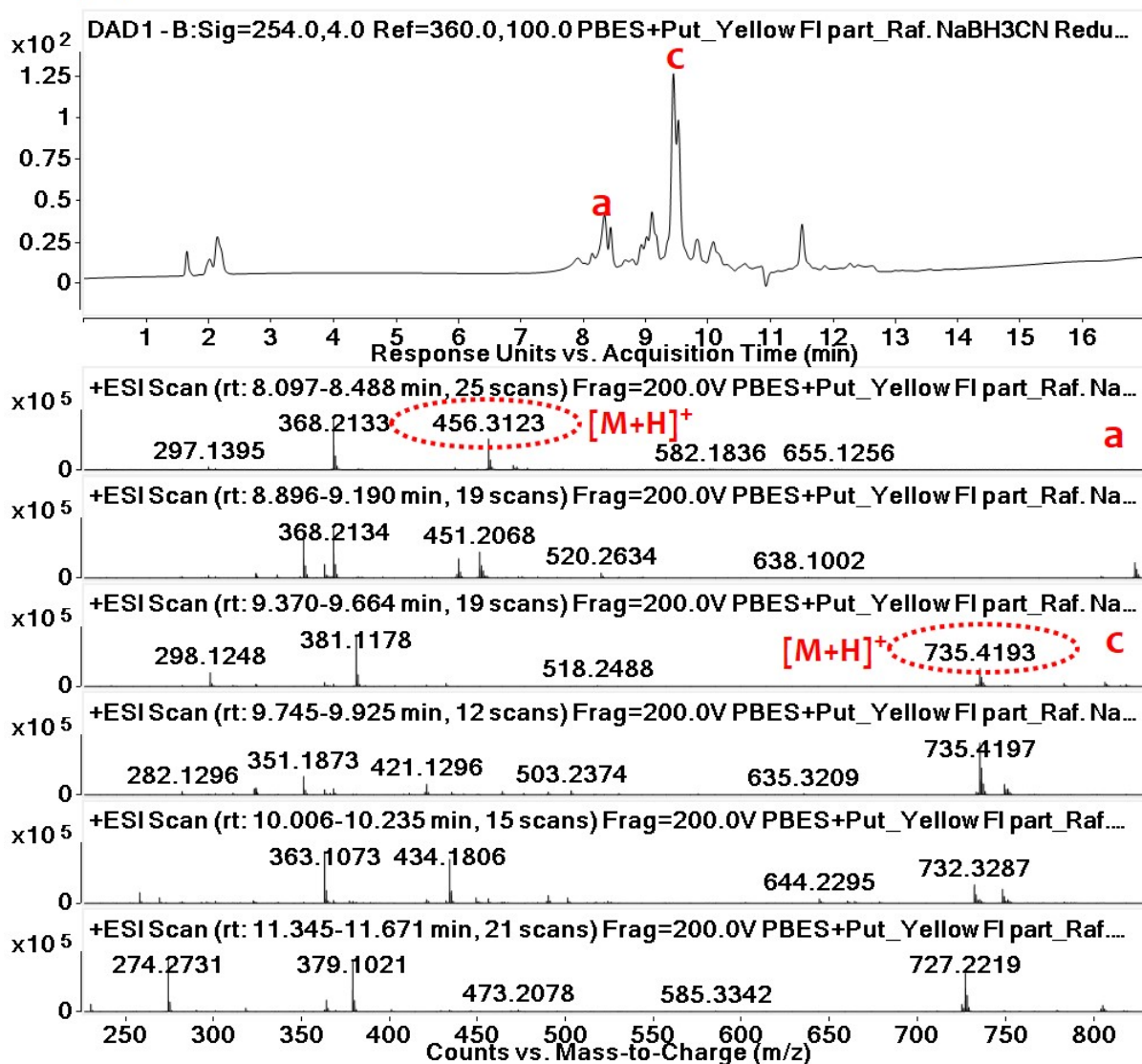
Figure S20. The partial ^1H NMR spectra taken from “**Figure S16**” for better visualization (a) $\delta = 4.8\text{--}3.0$ ppm, (b) $\delta = 5.0\text{--}4.0$ ppm, (c) $\delta = 8.5\text{--}6.1$ ppm.

4.2. LCMS profile for the reduction of **PBES-R** and **PBES-Y**:

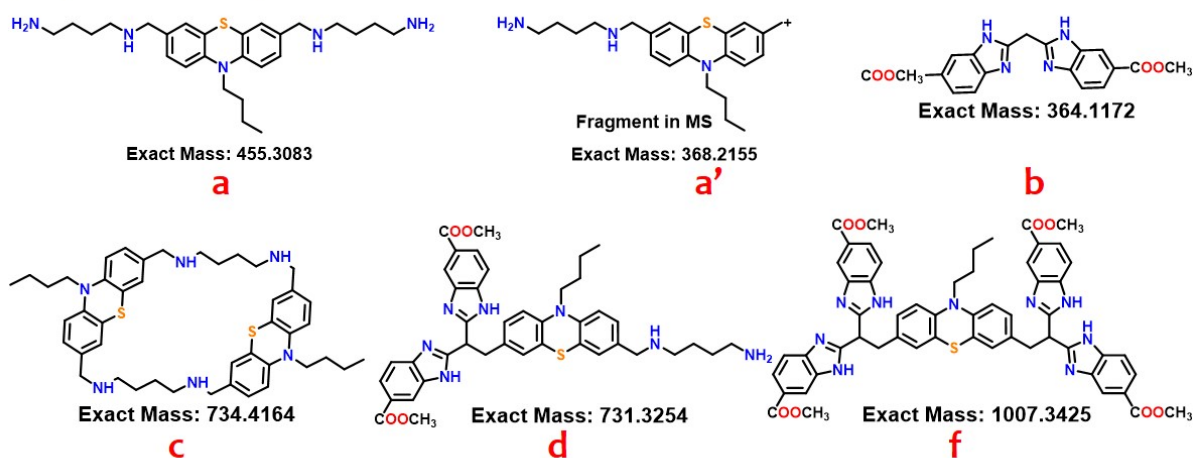
(i) Reduction of PBES-R



(ii). Reduction of PBES-Y



(iii). Structure predicted from LCMS data



(iv) Proposed mechanism

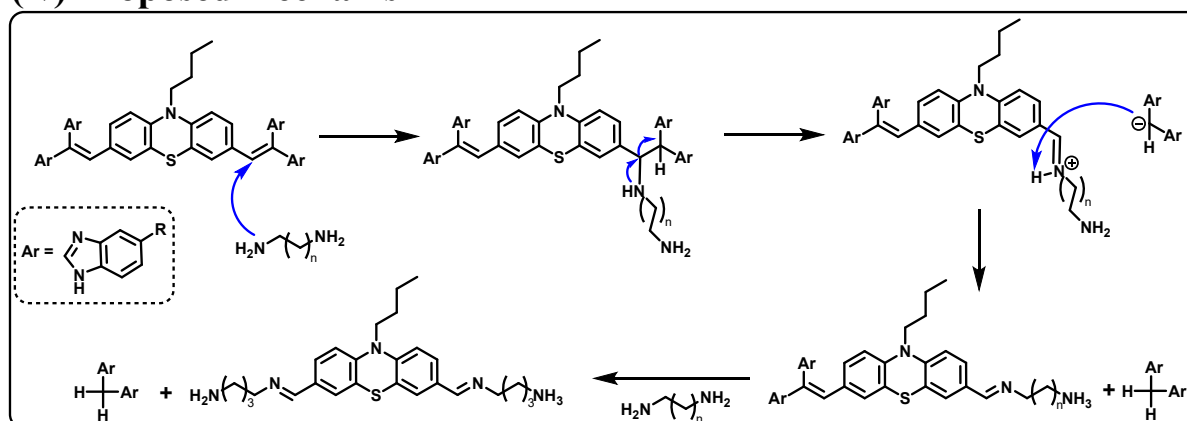


Figure S21. Analytical RP-HPLC profile (254 nm) of reduction of putrescine exposed state of compound PBES along with their ESI-LCMS data (i) PBES-R; (ii) PBES-Y, (iii) Chemical structure of the compound found after reduction of PBES-R, and PBES-Y with [NaBH₃(CN)] (predicted from the mass), (iv) Proposed mechanism. ‘e’ unidentified.

5. PXRD study for PBES, PBES-R, and PBES-Y

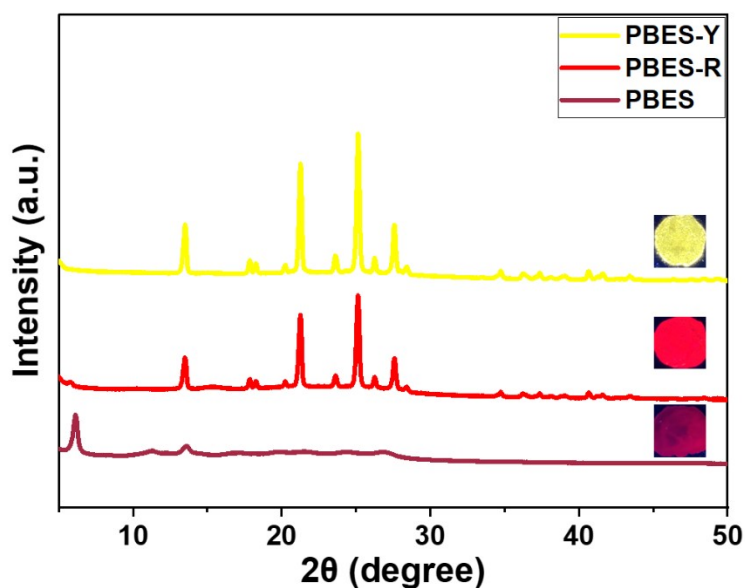
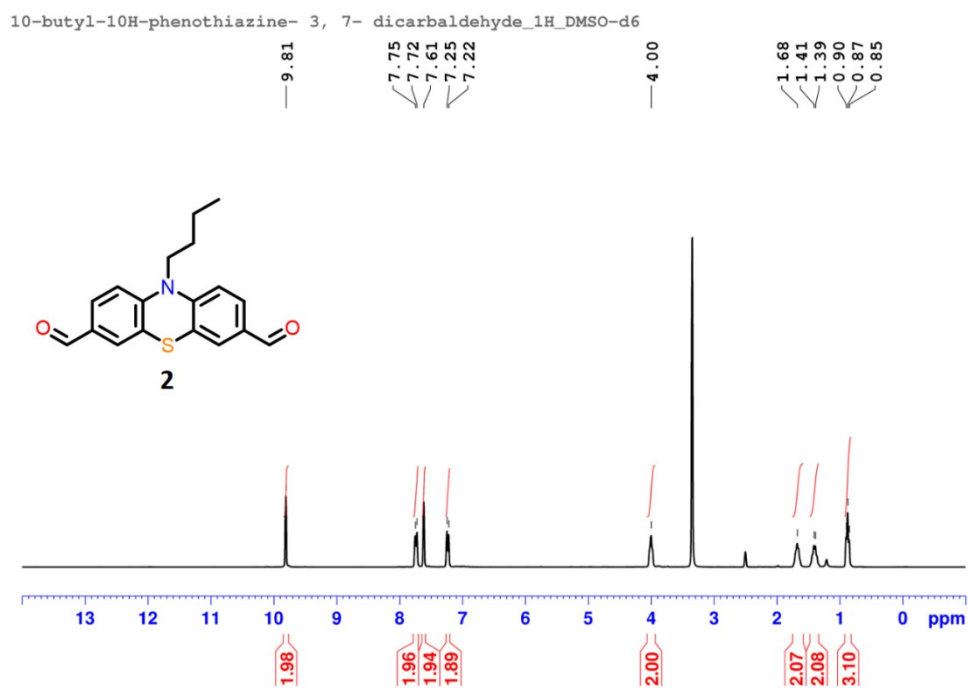


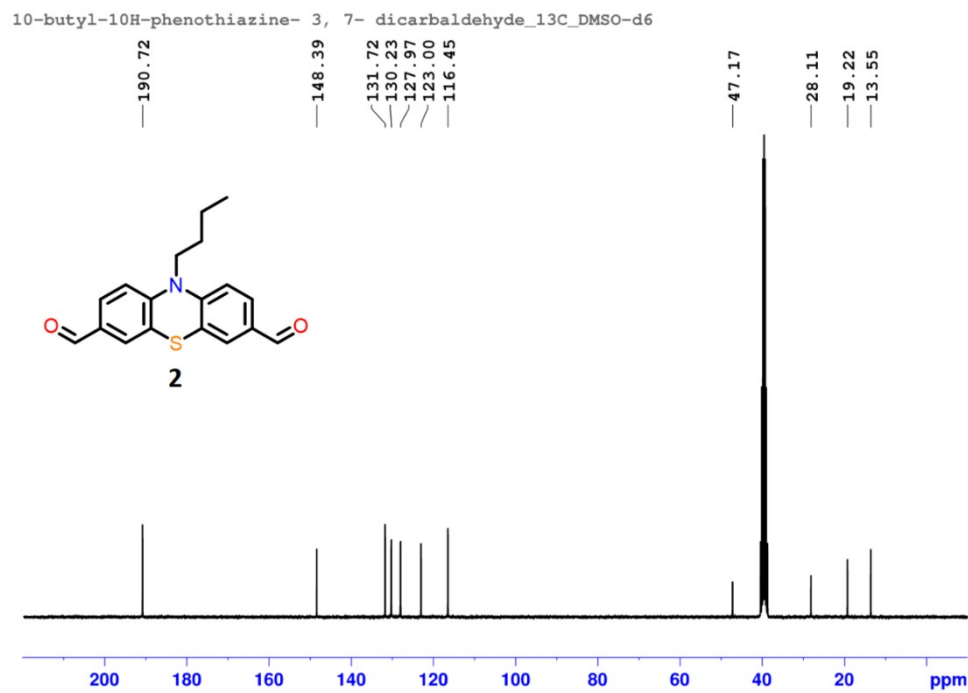
Figure S22. PXRD data of PBES, PBES-R, and PBES-Y.

6. NMR and HRMS data

(A)



(B)



(C)

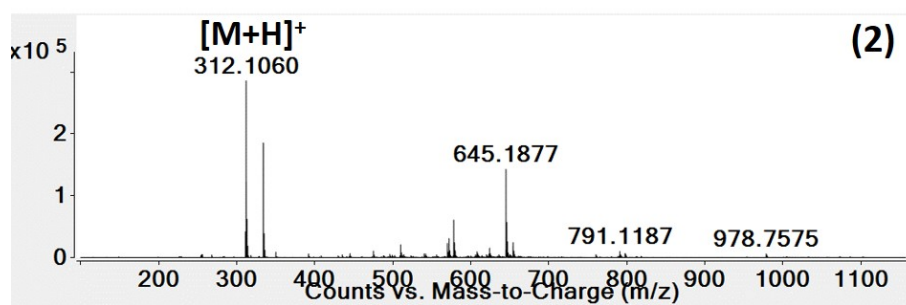
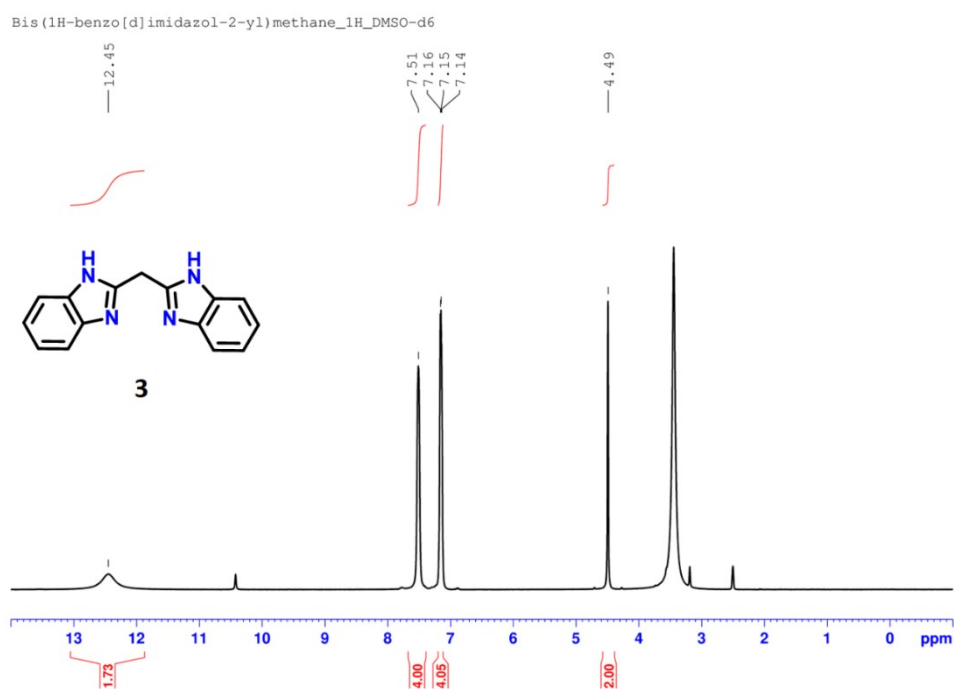
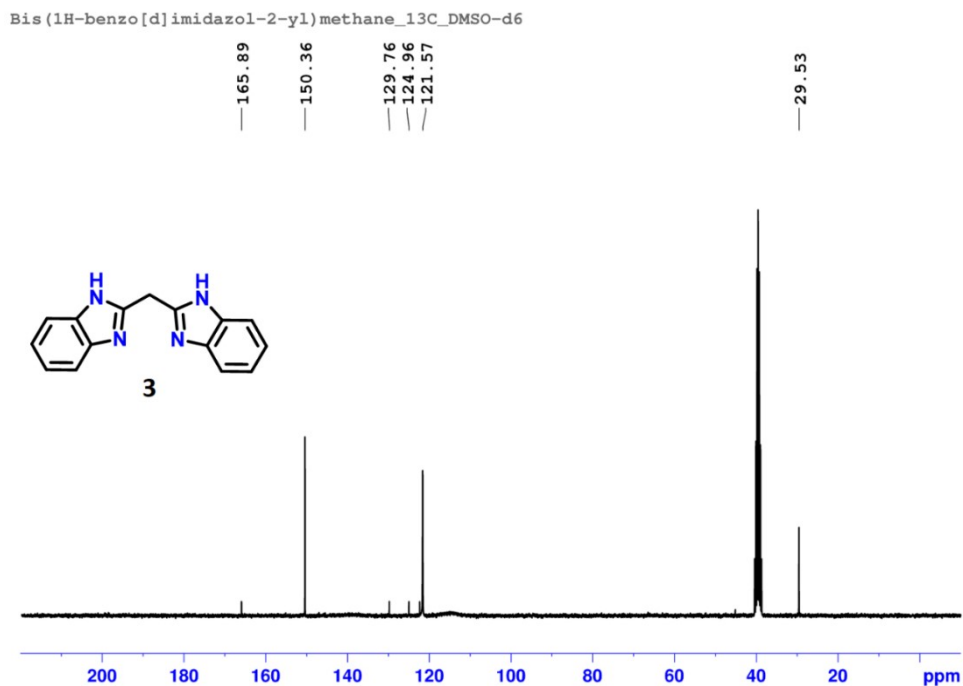


Figure S23. NMR, and HRMS data of 10-butyl-10H-phenothiazine-3,7-dicarbaldehyde (**2**). (A) ^1H -NMR (300 MHz, $\text{DMSO-}d_6$, 25 $^\circ\text{C}$). (B) $^{13}\text{C}\{^1\text{H}\}$ -NMR (75.5 MHz, $\text{DMSO-}d_6$, 25 $^\circ\text{C}$). (C) HRMS data.

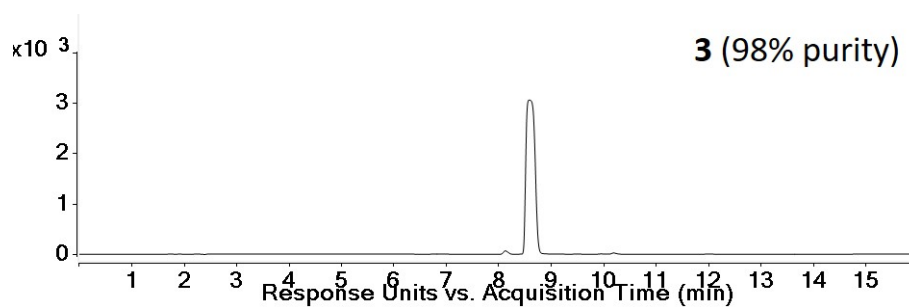
(A)



(B)



(C)



(D)

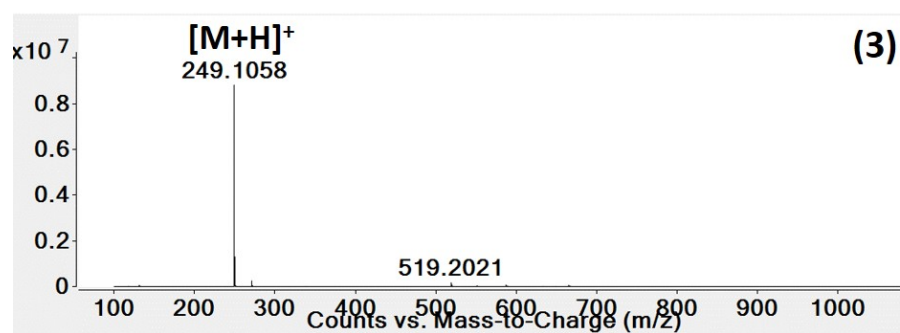
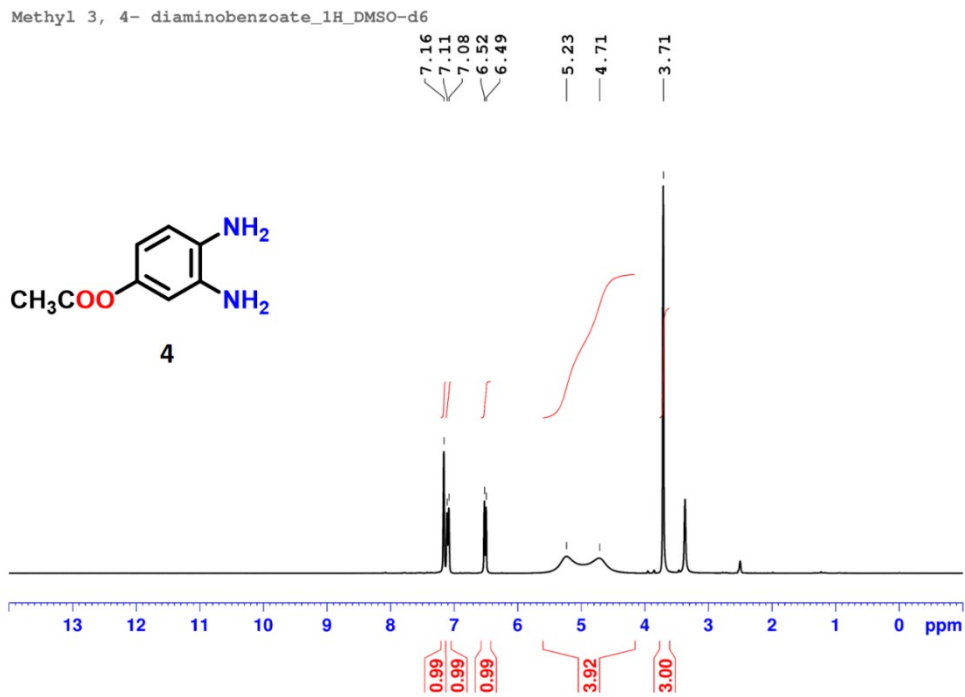
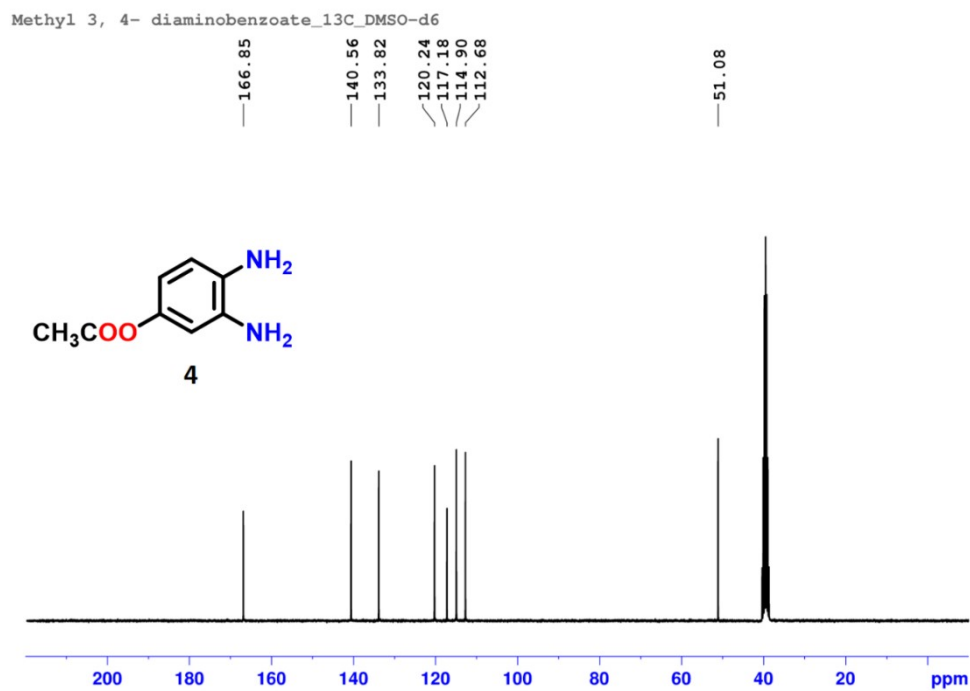


Figure S24. NMR, HPLC and HRMS data of **3**. (A) ^1H -NMR (300 MHz, $\text{DMSO-}d_6$, 25 °C), (B) $^{13}\text{C}\{^1\text{H}\}$ -NMR (75.5 MHz, $\text{DMSO-}d_6$, 25 °C). (C) HPLC chromatogram of pure compound. (D) HRMS data.

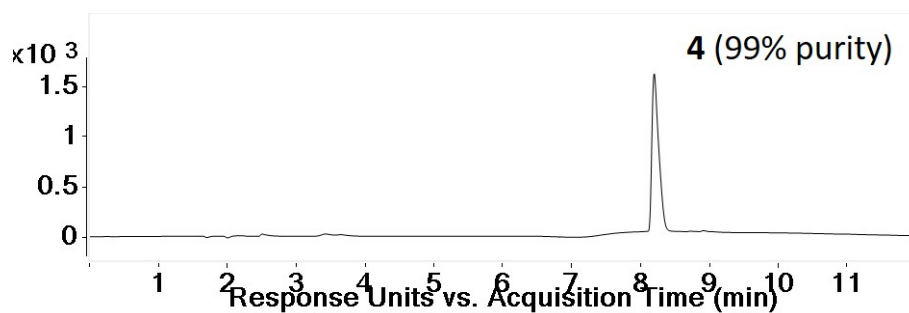
(A)



(B)



(C)



(D)

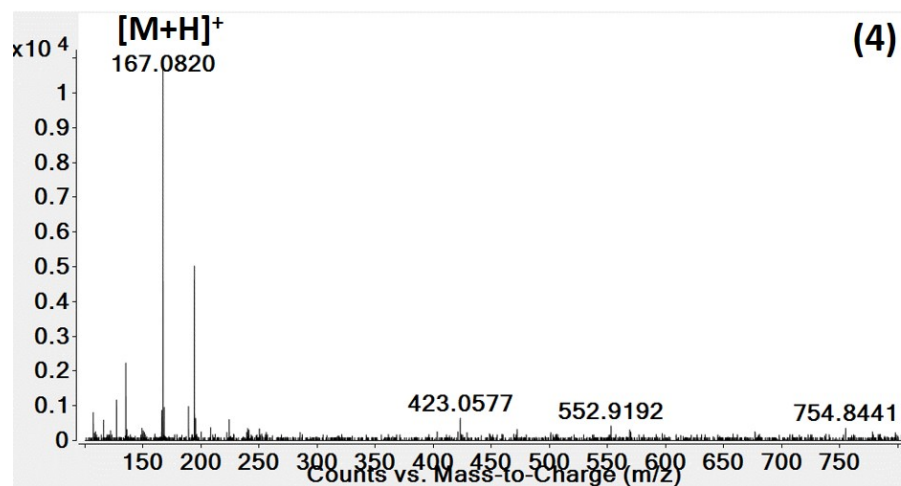
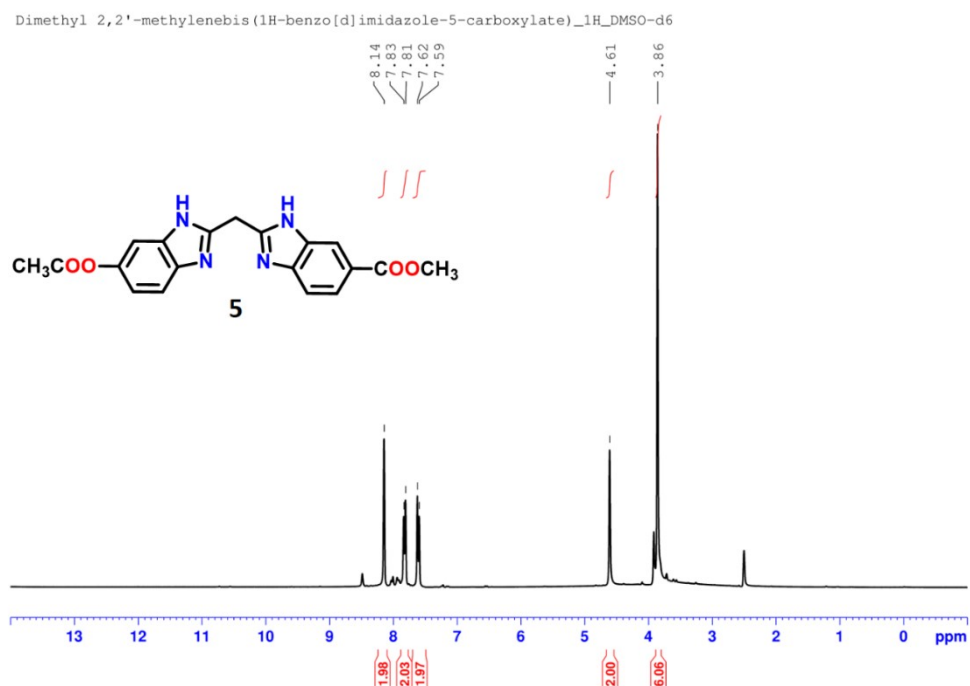
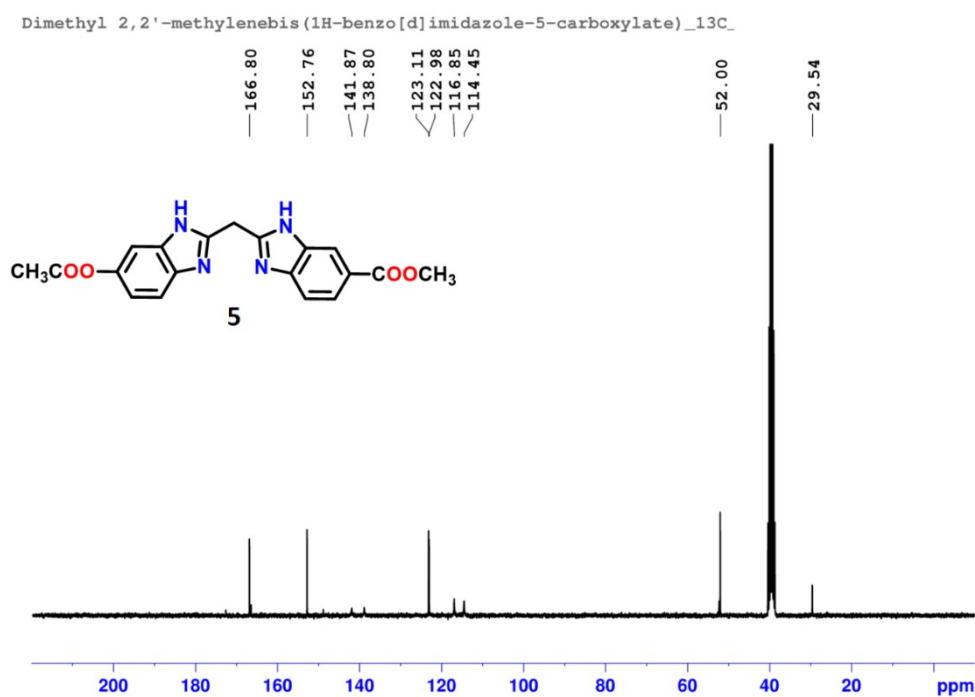


Figure S25. NMR, HPLC, and HRMS data of **(4)**. **(A)** ^1H -NMR (300 MHz, $\text{DMSO-}d_6$, 25 °C). **(B)** $^{13}\text{C}\{^1\text{H}\}$ -NMR (75.5 MHz, $\text{DMSO-}d_6$, 25 °C). **(C)** HPLC chromatogram of pure compound. **(D)** HRMS data.

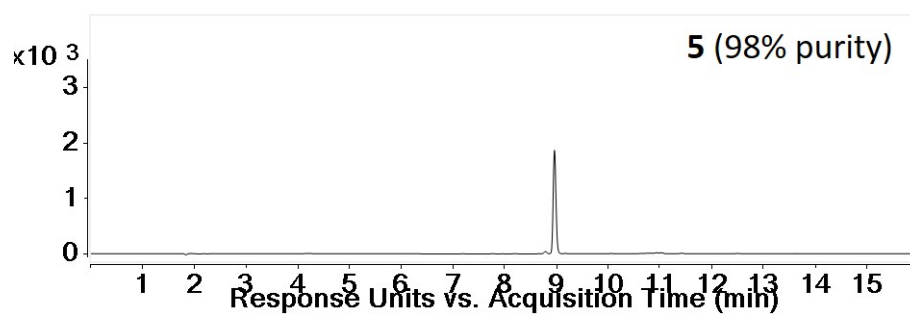
(A)



(B)



(C)



(D)

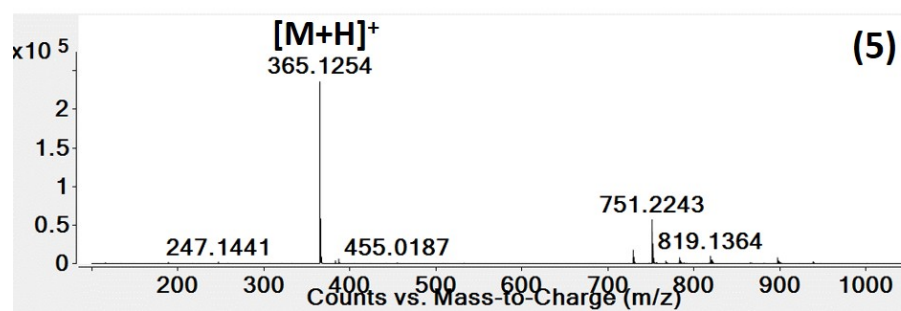
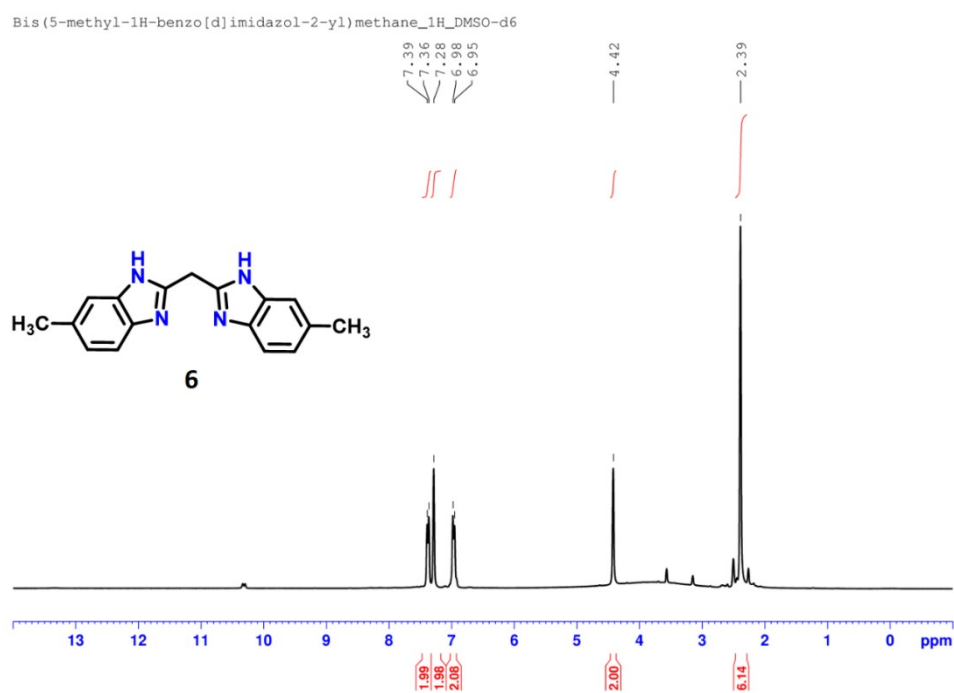
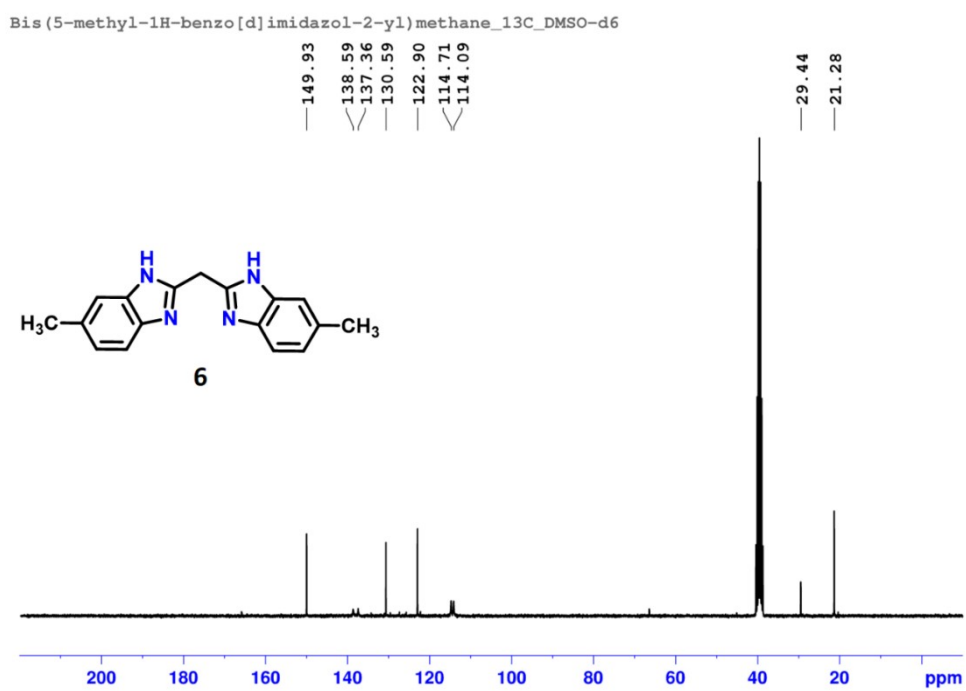


Figure S26. NMR, HPLC, and HRMS data of **5**. (A) ¹H-NMR (300 MHz, DMSO-*d*₆, 25 °C). (B) ¹³C{¹H}-NMR (75.5 MHz, DMSO-*d*₆, 25 °C). (C) HPLC chromatogram of pure compound. (D) HRMS data.

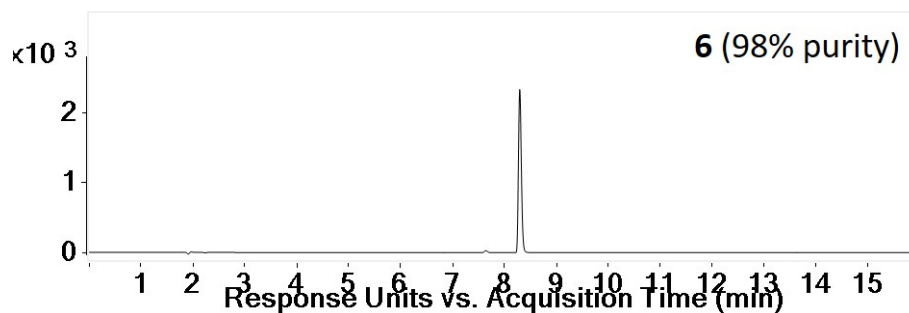
(A)



(B)



(C)



(D)

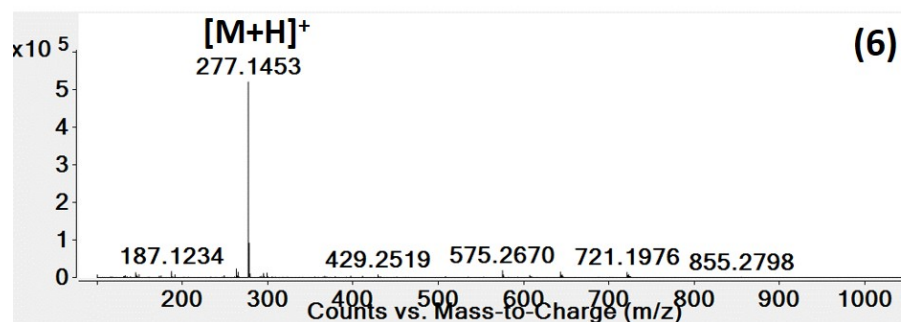
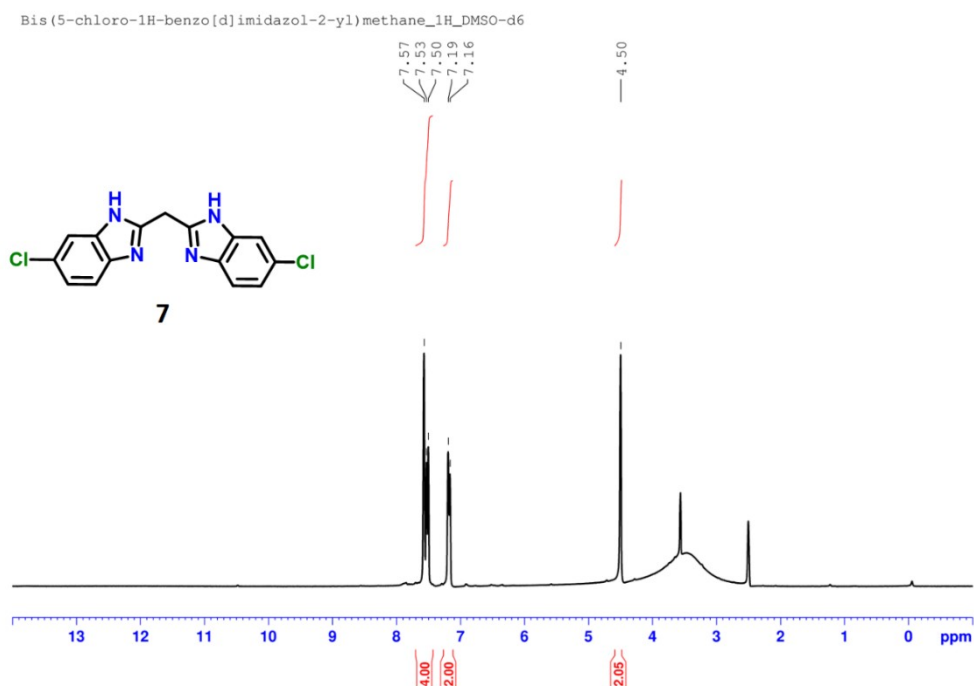
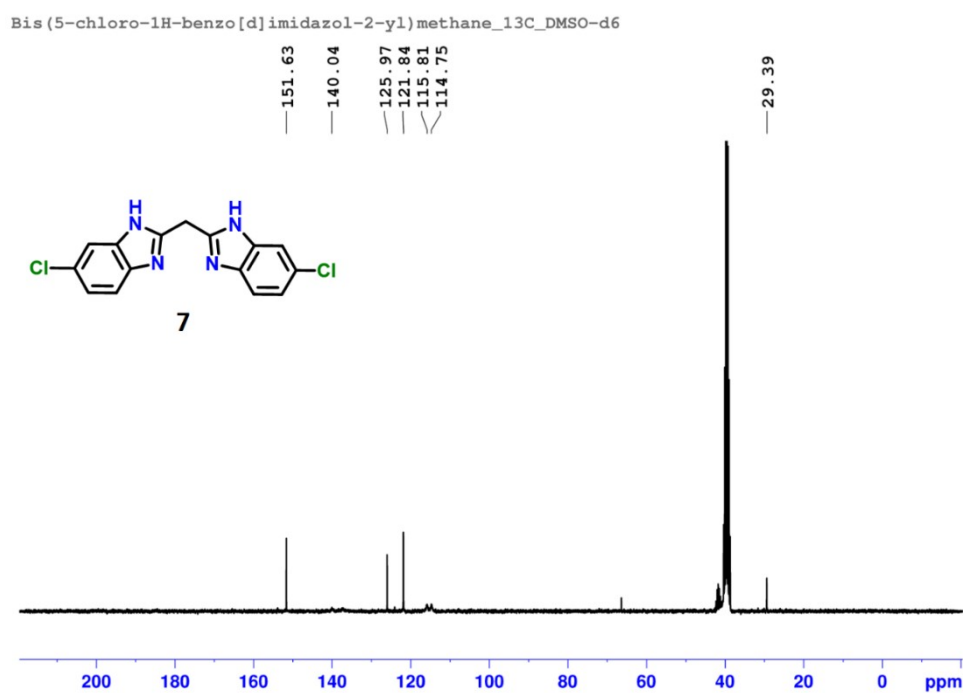


Figure S27. NMR, HPLC, and HRMS data of **6**. (A) ^1H -NMR (300 MHz, $\text{DMSO-}d_6$, 25 °C). (B) $^{13}\text{C}\{^1\text{H}\}$ -NMR (75.5 MHz, $\text{DMSO-}d_6$, 25 °C). (C) HPLC chromatogram of pure compound. (D) HRMS data.

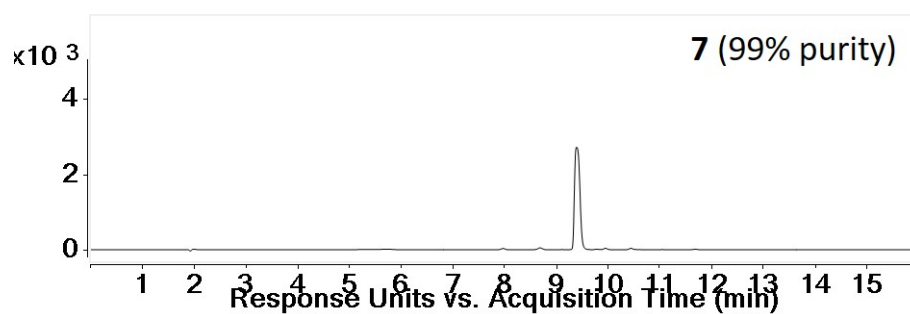
(A)



(B)



(C)



(D)

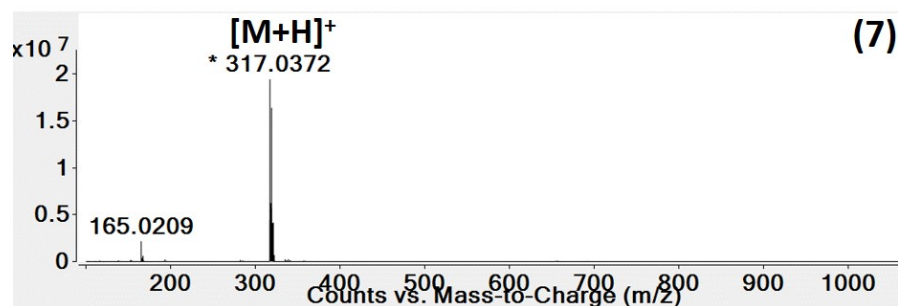
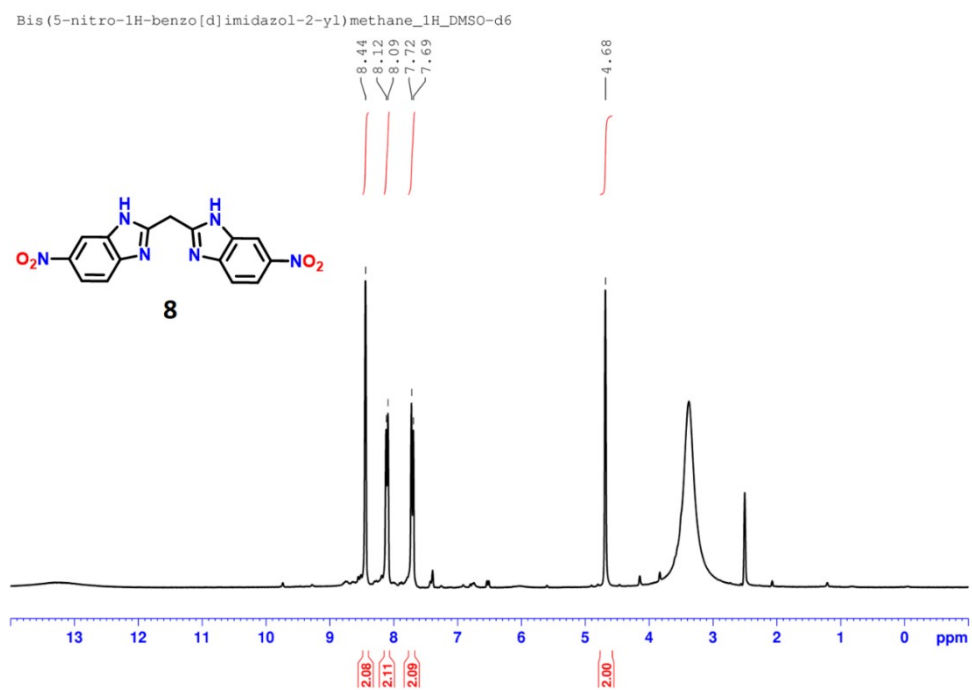
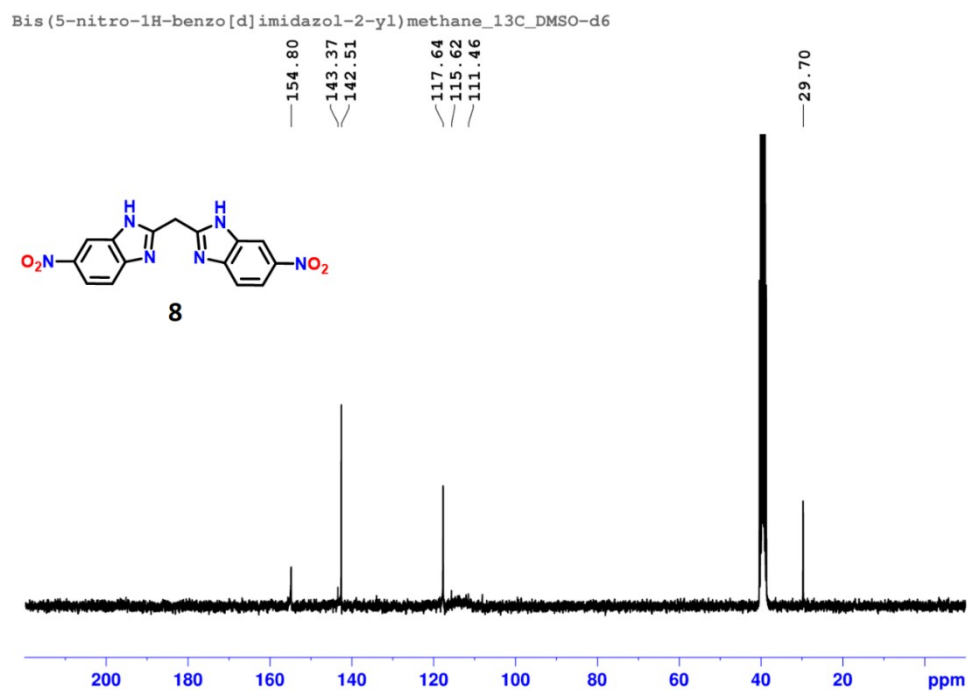


Figure S28. NMR, HPLC, and HRMS spectra of **7**. (A) ¹H-NMR (300 MHz, DMSO-*d*₆, 25 °C). (B) ¹³C{¹H}-NMR (75.5 MHz, DMSO-*d*₆, 25 °C). (C) HPLC chromatogram of pure compound. (D) HRMS data.

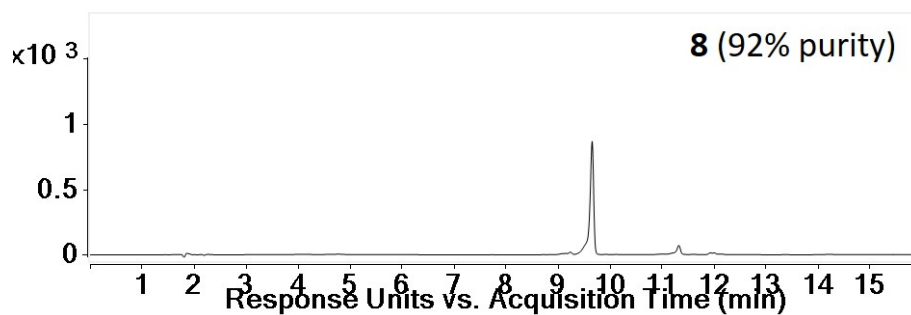
(A)



(B)



(C)



(D)

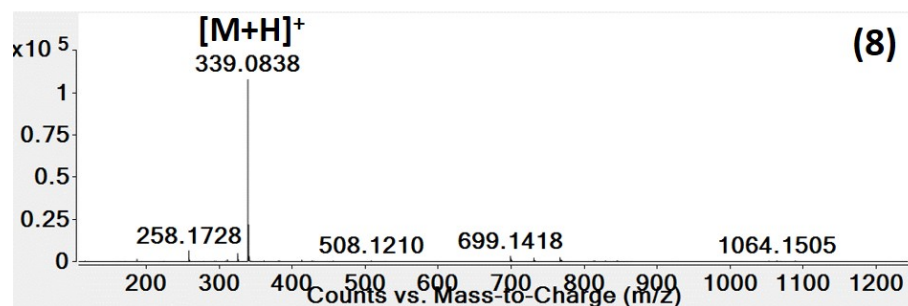
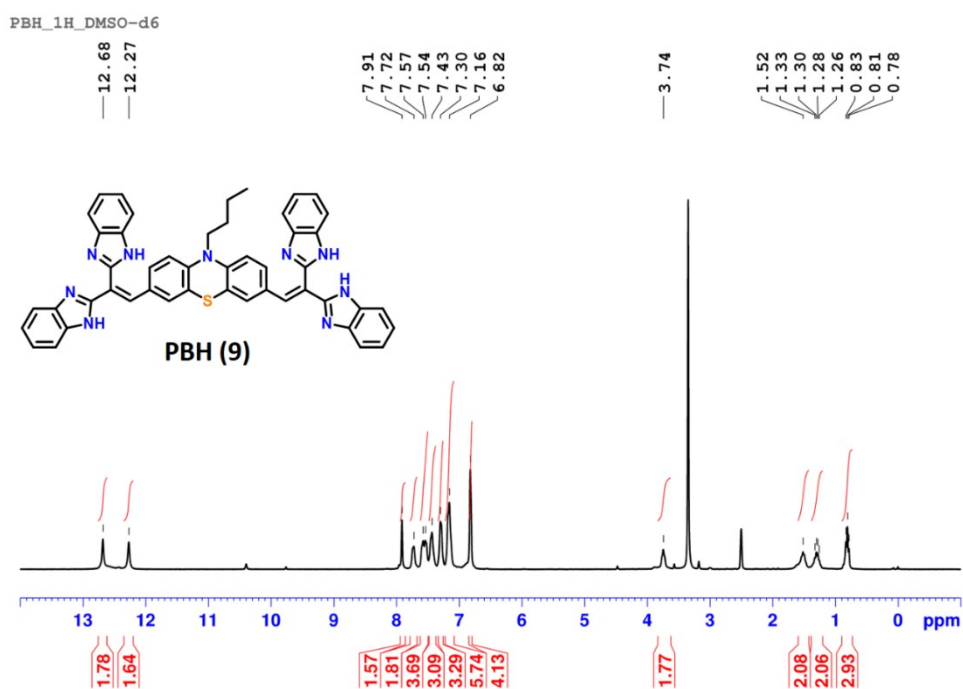
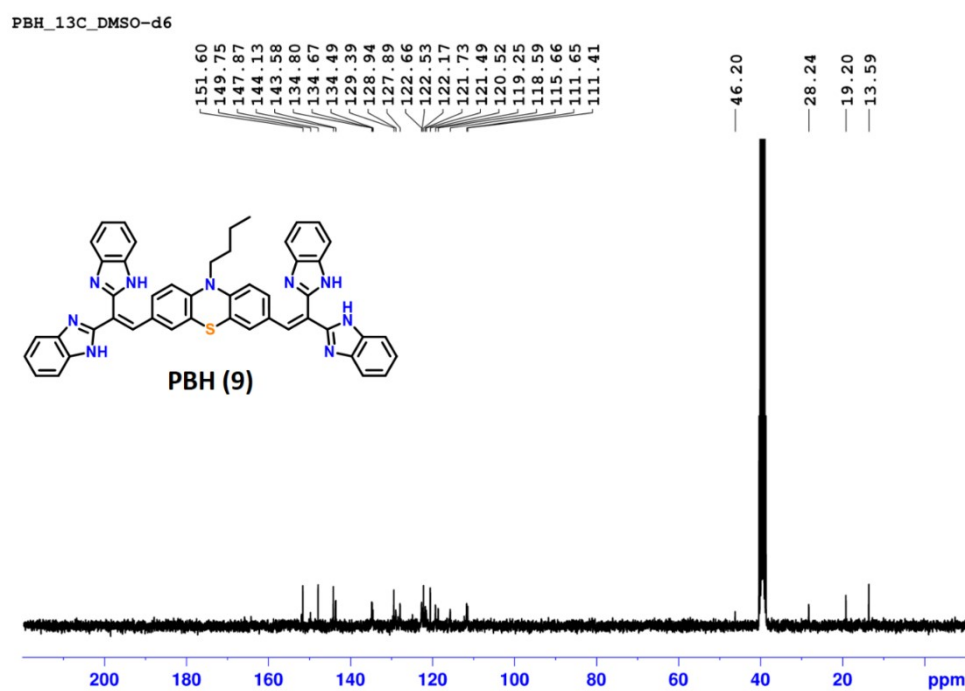


Figure S29. NMR, HPLC, and HRMS spectra of **8**. (A) ^1H -NMR (300 MHz, $\text{DMSO-}d_6$, 25 °C). (B) $^{13}\text{C}\{^1\text{H}\}$ -NMR (75.5 MHz, $\text{DMSO-}d_6$, 25 °C). (C) HPLC chromatogram of final compound. (D) HRMS data.

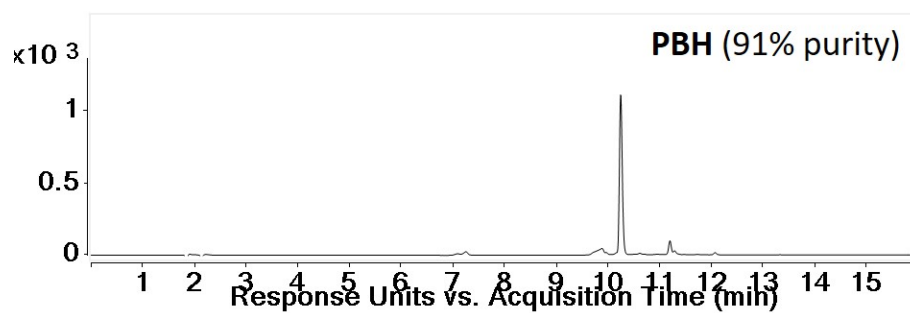
(A)



(B)



(C)



(D)

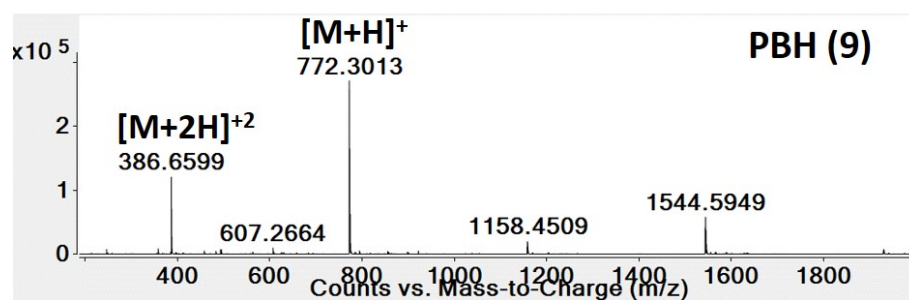
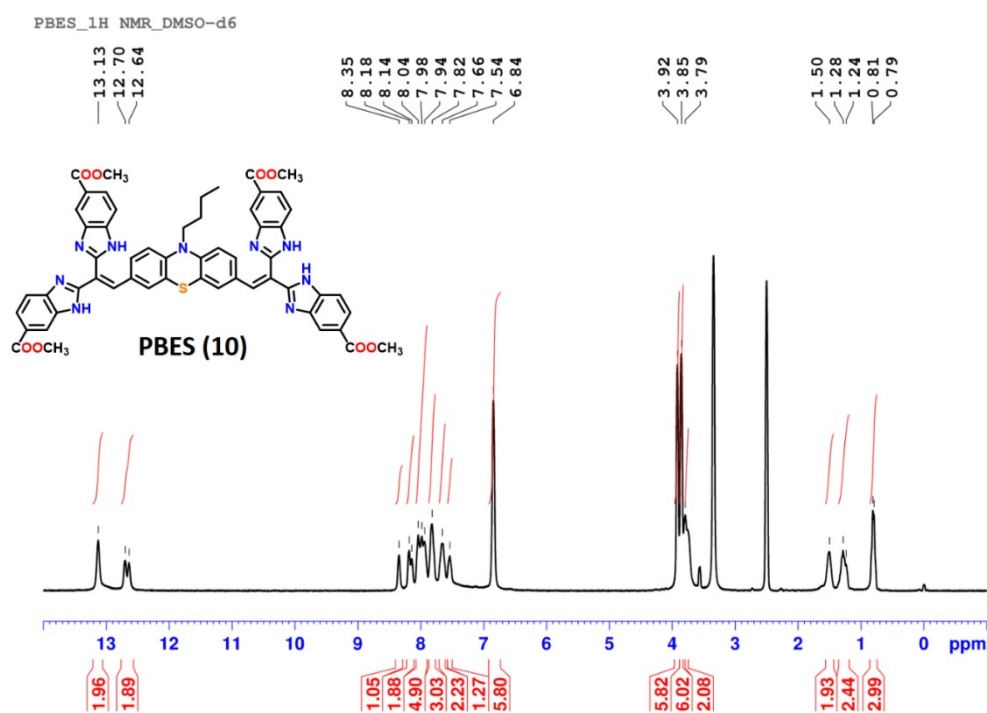
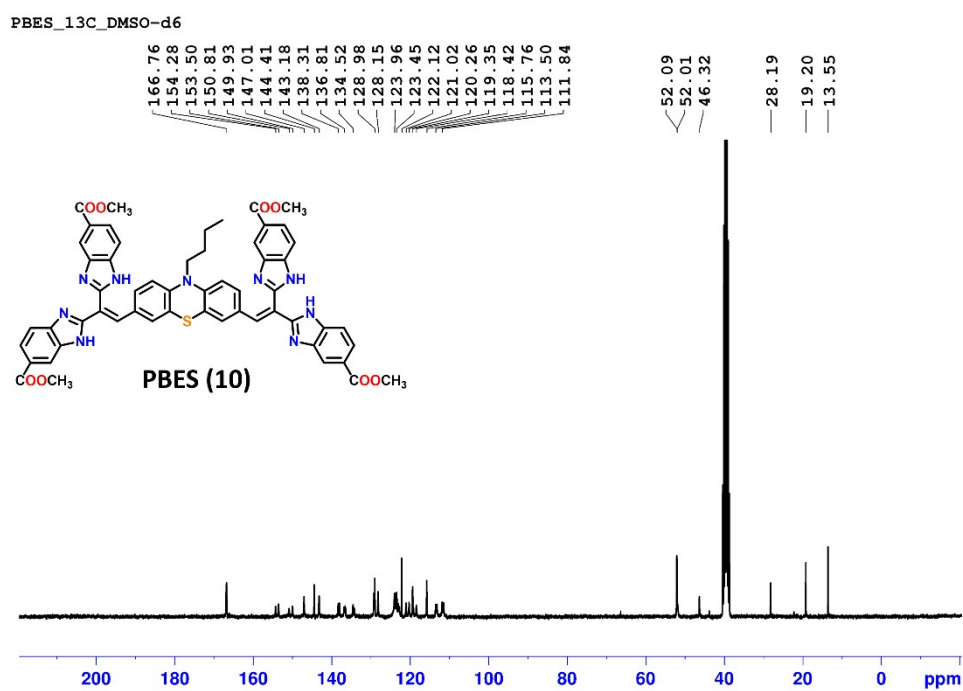


Figure S30. NMR, HPLC, and HRMS spectra of **PBH (9)**. (A) ^1H -NMR (300 MHz, $\text{DMSO-}d_6$, 25 °C). (B) $^{13}\text{C}\{^1\text{H}\}$ -NMR (75.5 MHz, $\text{DMSO-}d_6$, 25 °C). (C) HPLC chromatogram of final compound. (D) HRMS data.

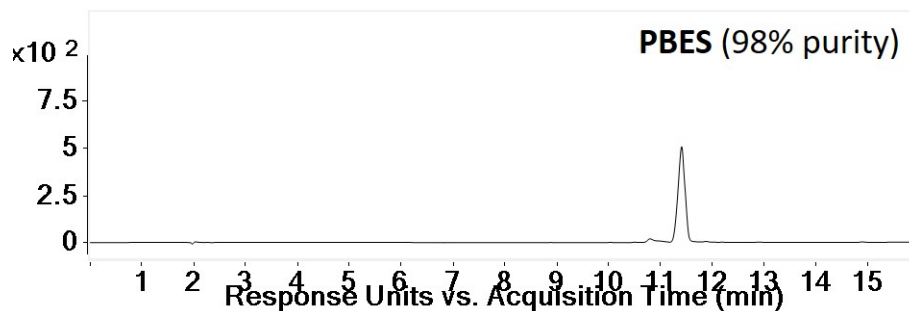
(A)



(B)



(C)



(D)

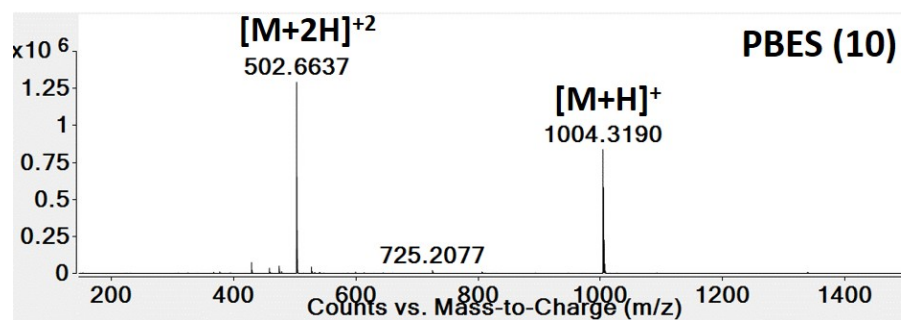
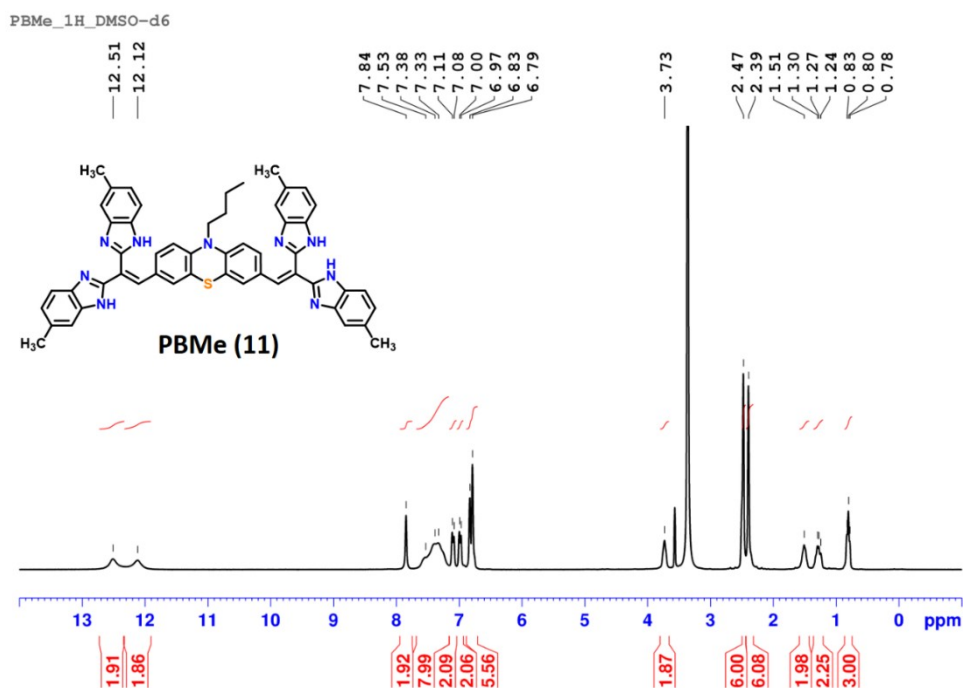
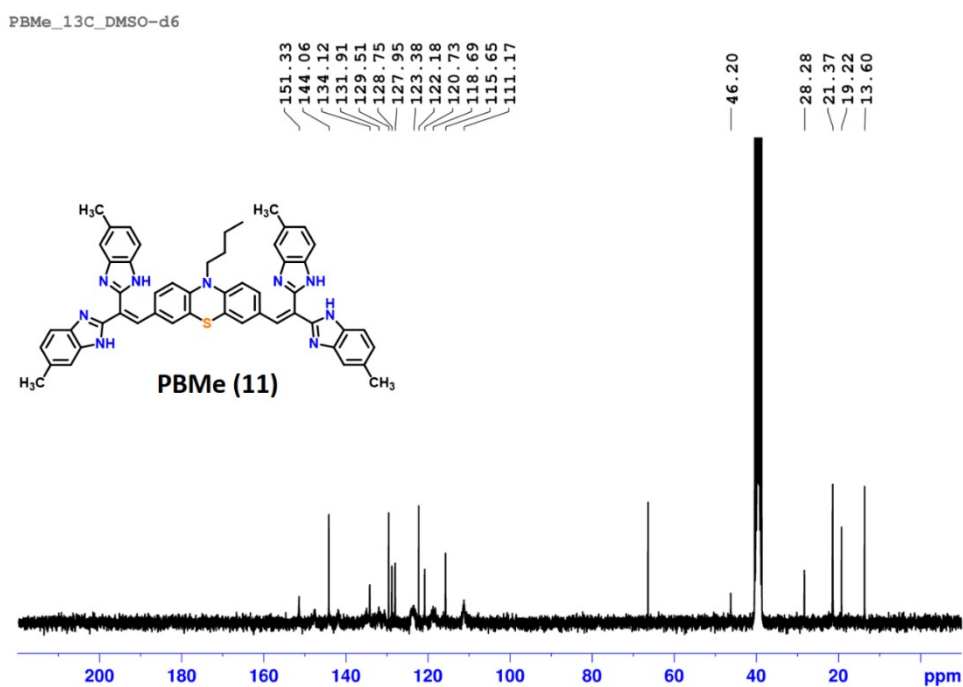


Figure S31. NMR, HPLC, and HRMS spectra of **PBES (10)**. (A) ^1H -NMR (300 MHz, $\text{DMSO-}d_6$, 25 °C). (B) $^{13}\text{C}\{^1\text{H}\}$ -NMR (75.5 MHz, $\text{DMSO-}d_6$, 25 °C), a little dioxane was noticed. (C) HPLC chromatogram of pure compound. (D) HRMS data.

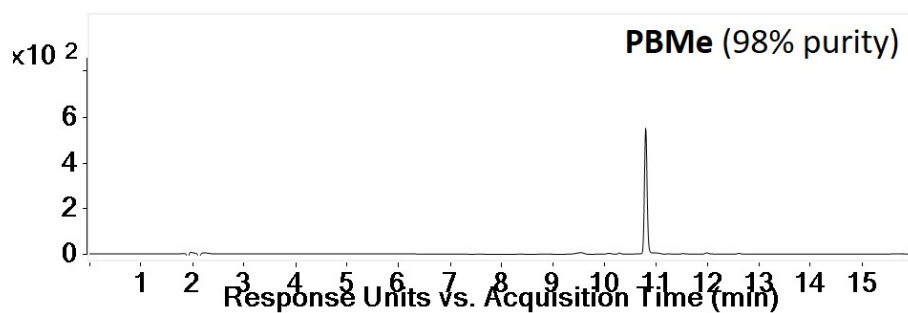
(A)



(B)



(C)



(D)

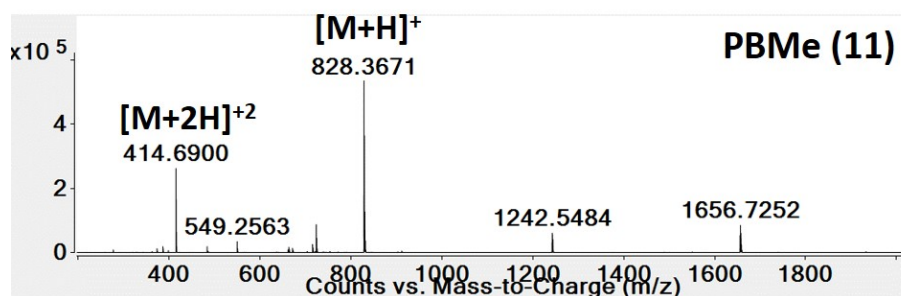
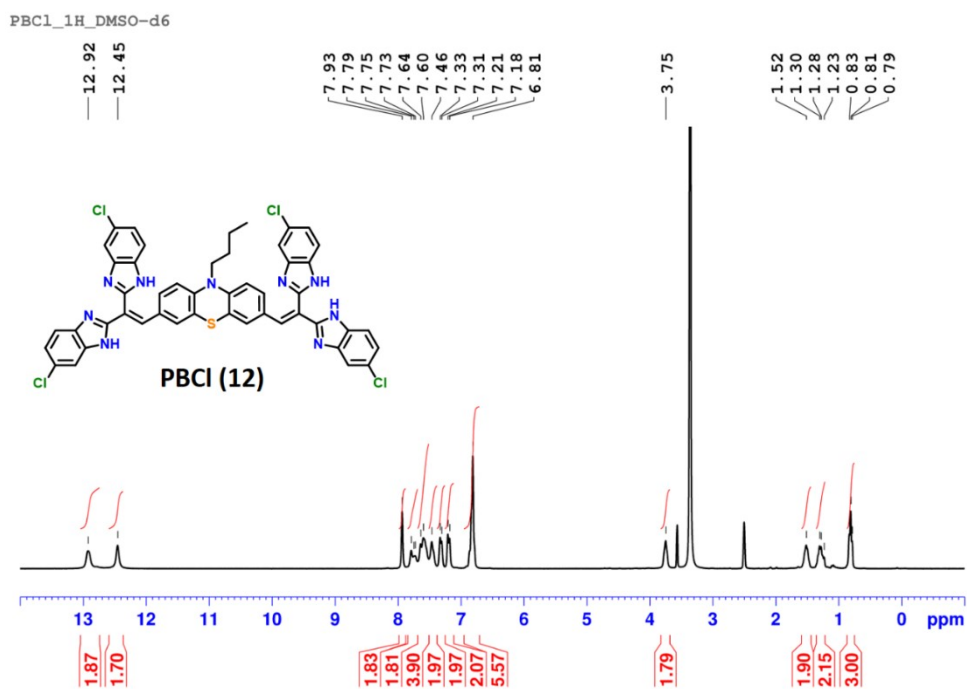
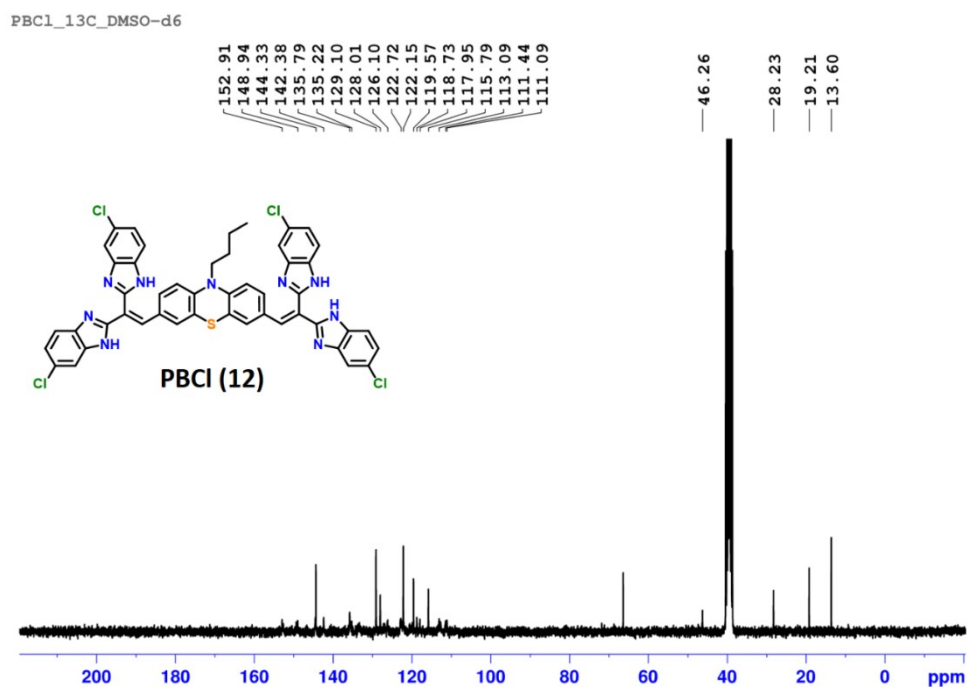


Figure S32. NMR, HPLC, and HRMS spectra of **PBMe (11)**. (A) ¹H-NMR (300 MHz, DMSO-*d*₆, 25 °C). (B) ¹³C{¹H}-NMR (75.5 MHz, DMSO-*d*₆, 25 °C). (C) HPLC chromatogram of pure compound. (D) HRMS data.

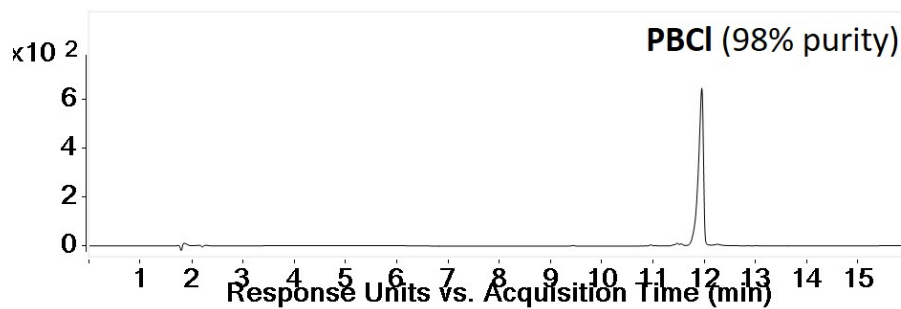
(A)



(B)



(C)



(D)

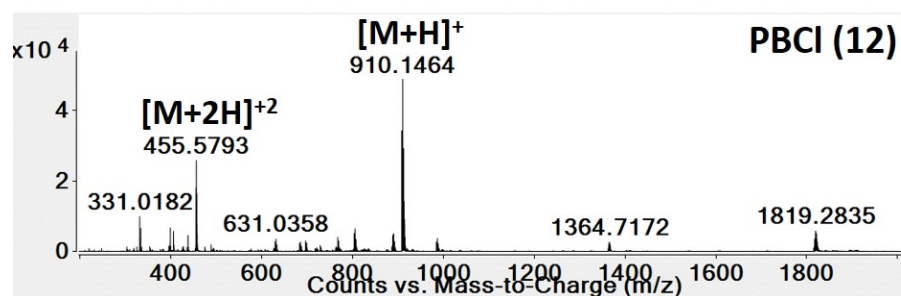
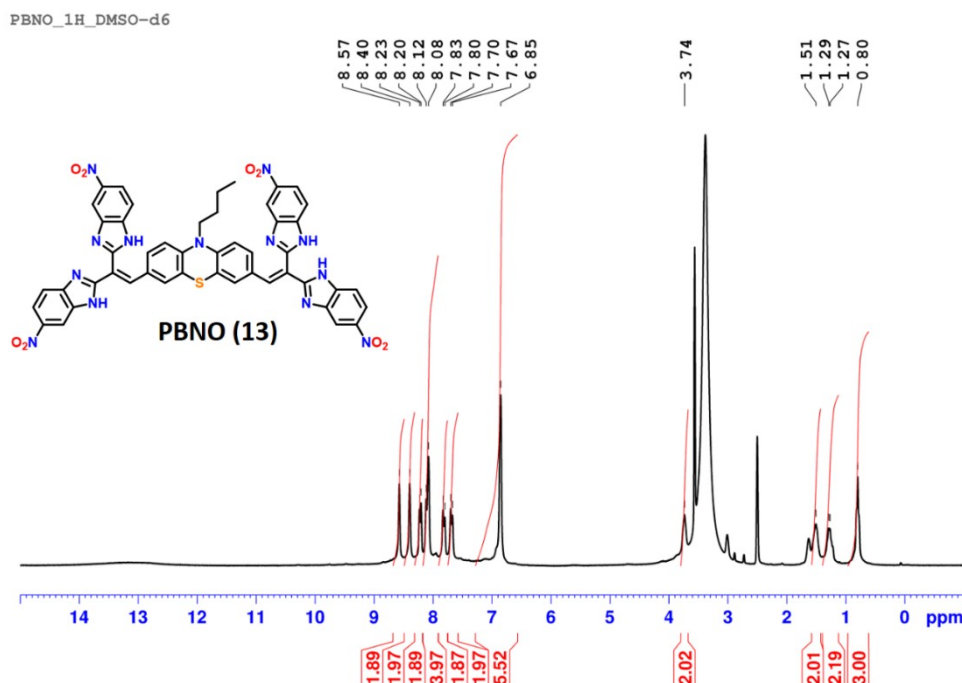
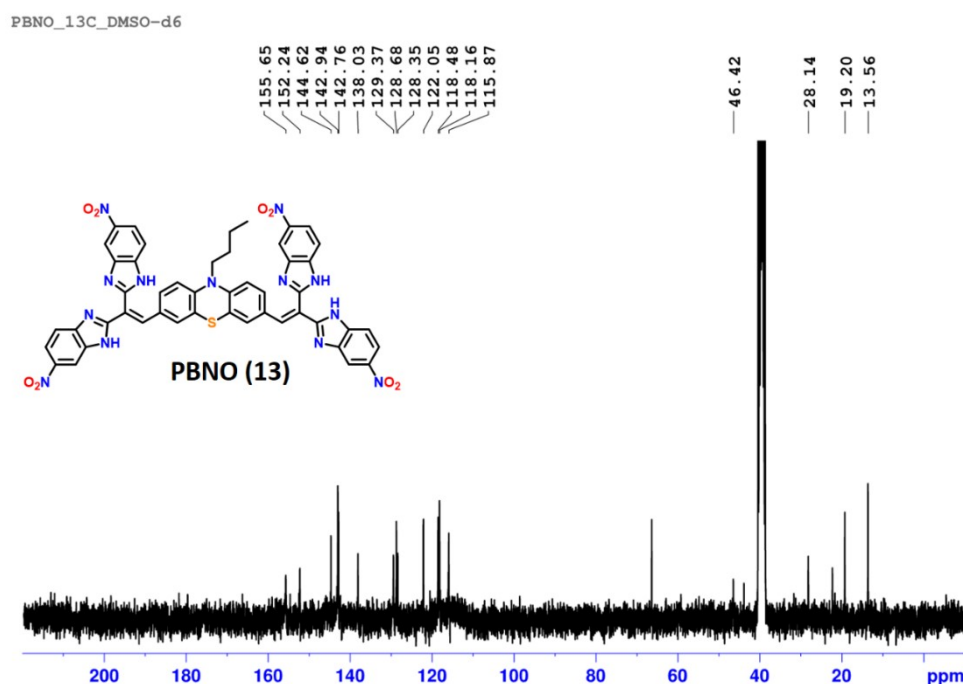


Figure S33. NMR, HPLC, and HRMS spectra of **PBCI (12)**. **(A)** ¹H-NMR (300 MHz, DMSO-*d*₆, 25 °C). **(B)** ¹³C{¹H}-NMR (75.5 MHz, DMSO-*d*₆, 25 °C). **(C)** HPLC chromatogram of pure compound. **(D)** HRMS data.

(A)



(B)



(C)

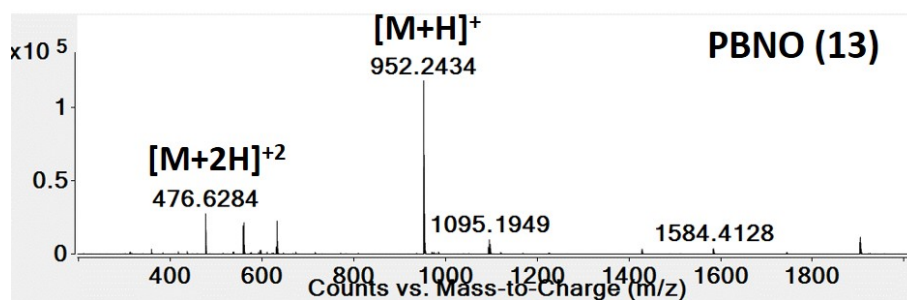


Figure S34. NMR, and HRMS spectra of **PBNO (13)**. **A)** ^1H -NMR (300 MHz, $\text{DMSO-}d_6$, 25 °C). **(B)** $^{13}\text{C}\{^1\text{H}\}$ -NMR (75.5 MHz, $\text{DMSO-}d_6$, 25 °C). **(C)** HRMS data.

7. References

1. Mallegol, T.; Gmouh, S.; Meziane, M. A. A.; Blanchard-Desce, M.; Mongin, O. *Synthesis* **2005**, *11*, 1771–1774.
2. Kattimani, P. P.; Kamble, R. R.*; Meti, G. Y. *RSC Adv.* **2015**, *5*, 29447–29455.
3. Gaussian 09, Revision D.01, M. J. Frisch, G. W. Trucks, H. B. Schlegel, G. E. Scuseria, M. A. Robb, J. R. Cheeseman, G. Scalmani, V. Barone, B. Mennucci, G. A. Petersson, H. Nakatsuji, M. Caricato, X. Li, H. P. Hratchian, A. F. Izmaylov, J. Bloino, G. Zheng, J. L. Sonnenberg, M. Hada, M. Ehara, K. Toyota, R. Fukuda, J. Hasegawa, M. Ishida, T. Nakajima, Y. Honda, O. Kitao, H. Nakai, T. Vreven, J. A. Montgomery, Jr., J. E. Peralta, F. Ogliaro, M. Bearpark, J. J. Heyd, E. Brothers, K. N. Kudin, V. N.

Staroverov, T. Keith, R. Kobayashi, J. Normand, K. Raghavachari, A. Rendell, J. C. Burant, S. S. Iyengar, J. Tomasi, M. Cossi, N. Rega, J. M. Millam, M. Klene, J. E. Knox, J. B. Cross, V. Bakken, C. Adamo, J. Jaramillo, R. Gomperts, R. E. Stratmann, O. Yazyev, A. J. Austin, R. Cammi, C. Pomelli, J. W. Ochterski, R. L. Martin, K. Morokuma, V. G. Zakrzewski, G. A. Voth, P. Salvador, J. J. Dannenberg, S. Dapprich, A. D. Daniels, O. Farkas, J. B. Foresman, J. V. Ortiz, J. Cioslowski, and D. J. Fox, Gaussian, Inc., Wallingford CT, **2013**.